FLEXURAL VIBRATIONS OF ROTATING SHAFTS BY TRANSFER FINITE ELEMENT METHOD

A Thesis Submitted
In Partial Fulfilment of the Requirements
for the Degree of

MASTER OF TECHNOLOGY

by
KUNJUMON E. MATHEW

to the

DEPARTMENT OF MECHANICAL ENGINEERING
INDIAN INSTITUTE OF TECHNOLOGY, KANPUR
FEBRUARY, 1992

CERTIFICATE

This is to certify that the work entitled, Flexural Vibrations of Rotating Shafts by Transfer Finite Element Method, by Lt. Kunjumon E. Mathew has been carried out under my supervision and has not been submitted elsewhere for a degree.

Bhupinder Pal Singh. Feb 17, 92

(Bhupinder Pal Singh)
Professor
Mechanical Engineering Dept.
Indian Institute of Technology,
Kanpur 208 016

February, 1992

ACKNOWLEDGEMENT

I am deeply grateful to Dr. B.P. Singh, Professor, Department of Mechanical Engineering, IIT Kanpur, without whose patient guidance this report would not have been made feasible. I would also like to thank Dr. N.S. Vyas, Assistant Professor, Mechanical Engineering Dept. for his valuable help and assistance rendered during the course of preparation of this thesis work. I am also indepted to Philip Koshy, T.I. Ignatius, C. George John and Jacob Philips for their timely help at the hour of need.

Last, but not the least, I would like to thank my wife and son for their patience and motivation in making this report a reality.

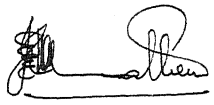

(Kunjumon E. Mathew)

February, 1992

CONTENTS

consistent mass approach over estimates frequencies while lumped mass approach under estimates. Difference could also be due to the fact that bearing properties used in the present work may be different from those of [17] (not given).

4.6 UNBALANCE RESPONSE

Unbalance response of a steel shaft carrying a disk at the centre supported in elastic bearings at both ends, shown in Fig. (4.2) with an unbalance of 5 kg-mm at the mid plane of the disk is studied. Both the disk and shaft are assumed to be of the same material having a density of 7833 kg/m^3 and Young's modulus of 206.8 GPa.

Unbalance response was studied for different bearing properties as shown in Table 13.

The results obtained are plotted in two graphs for each case under study. The first graph shows amplitude of whirl against shaft spin speed and second the whirl orbit of the shaft at 0.783 (6000 rpm). The results are shown in Figs. (4.3) to (4.12).

From the unbalance response of shafts, the following observations are made:

(a) With no damping the system becomes unstable at critical speed.

(b) External damping when introduced, either from medium or from bearing, the system stability is increased and whirl amplitudes decreases.

LIST OF TABLES

Table 4.13: Support Bearing Properties for Various Cases of Unbalance Study

Case	K_{xx}	K_{xy}	K_{yx}	K_{yy}	C_{xx}	C_{xy}	C_{yx}	C_{yy}	Dc
1	35.1	0.0	0.0	35.1	0.0	0.0	0.0	0.0	0.0
2	35.1	0.0	0.0	35.1	0.0	0.0	0.0	0.0	0.1
3	35.1	0.0	0.0	35.1	0.269	0.0	0.0	0.269	0.1
4	35.1	17.55	-17.55	35.1	0.269	0.134	0.134	0.269	0.1
5 LH	35.1	0.0	0.0	35.1	0.269	0.0	0.0	0.269	0.1
5 RH	70.2	0.0	0.0	70.2	0.538	0.0	0.0	0.538	

LIST OF FIGURES

NOMENCLATURE

A	Area of cross-section
A_o	Area of cross-section at s = 0.
[AB1],[AB2] ... [AB6]	Sub matrices of finite element coefficient matrix.
[AI]	Imaginary part of finite element coefficient matrix.
[AR]	Real part of finite element coefficient matrix.
c	External viscous damping due to resistance by medium.
$[C]^{(e)}$	Elemental damping matrix.
C_{xx}, C_{yy}. C_{yx}, C_{xy}	Non-dimensional bearing damping coefficients.
C1, C3	Non-dimensionalisation factors
D_c	Non-dimensional external viscous damping.
e	Eccentricity of unbalance.
E	Young's modulus.
E_o	Young's modulus at s = 0.
{EF}	Force vector due to unbalance.
F	Force
$[G]^{(e)}$	Elemental gyroscopic matrix.
H	Non-dimensional element length.
I	Moment of inertia about neutral axis.
I_o	Moment of inertia about neutral axis at s = 0.
I_p	Polar moment of inertia.
k	Radius of gyration.
k'	Shear deformation factor.
$[K]^{(e)}$	Elemental stiffness matrix.

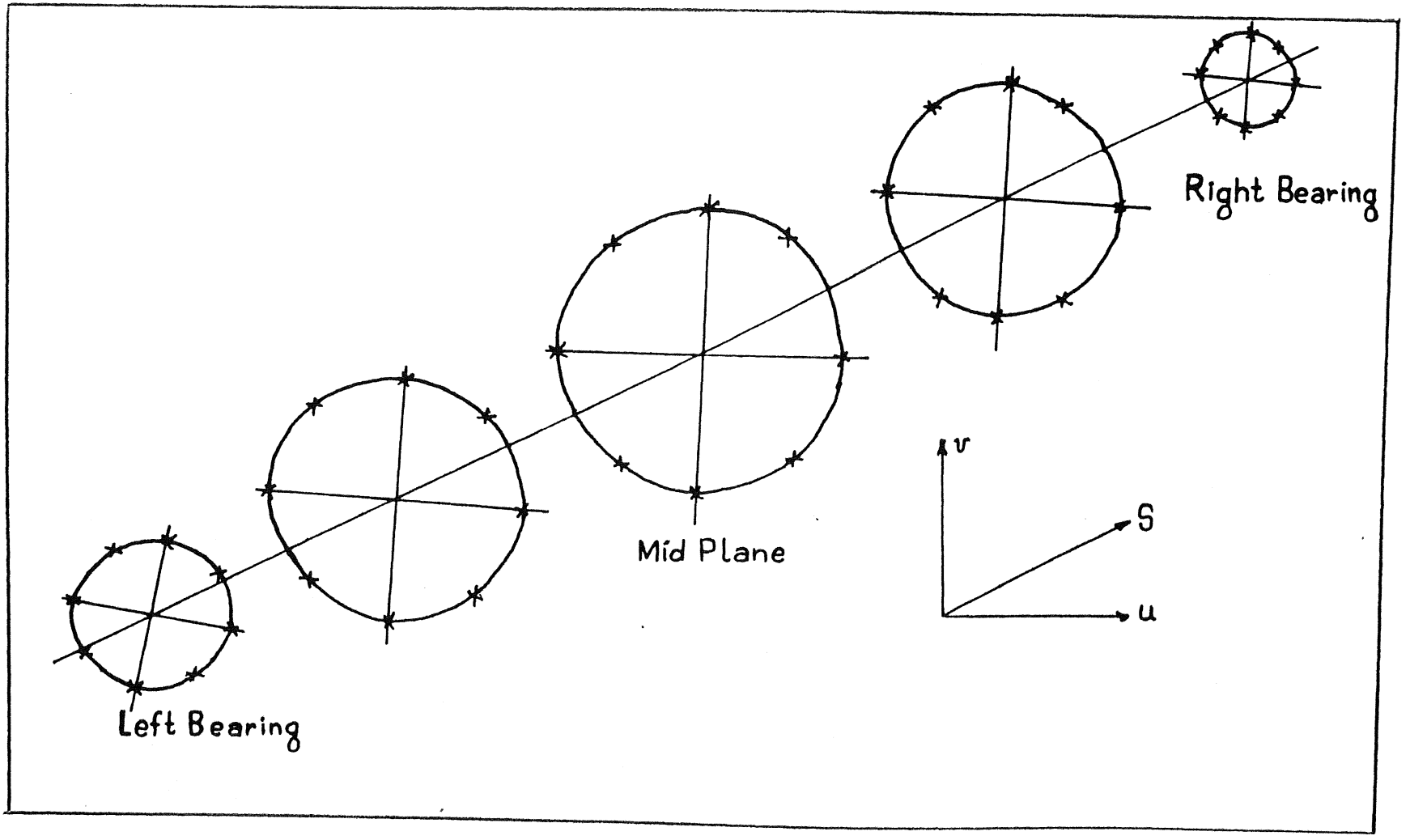

Fig. 4·12 Whirl Orbit At 6000 rpm (Case 5)

K_{xx}, K_{yy}, K_{yx}, K_{xy}	Non-dimensional bearing stiffnesses.
l	Elemental length.
L	Length between supports .
$[M]^{(e)}$	Elemental mass matrix.
M_c	Material constant.
MX	Bending moment about x-axis.
MY	Bending moment about y-axis.
[OT]	Overall finite element transfer matrix.
$\{p\}^{(ne)}$	Nodal displacements, bending slopes vector.
$\{q\}^{(ne)}$	Nodal displacements, bending slopes vector.
Q_x	Shear force along x-axis.
Q_y	Shear force along y-axis.
{Q}	Unbalance force vector.
Re	Rotary inertia coefficient
t	Time.
T	Non-dimensional time.
T*	Non-dimensionalisation factor.
$[T]^{(e)}$	Elemental finite element transfer matrix.
T_e	Kinetic energy.
U	Translational displacement of geometric centre along x-axis.
u	Non-dimensional displacement.
U_e	Strain energy.
U_g	Translational displacement of centre of mass along x-axis.
V	Translational displacement of geometriccentre along y-axis.

14. Mahendrakar, V, "Critical Speeds and Stability of Rotating Shafts by FEM", M. Tech. Thesis, Department of Mechanical Engg., IIT, Kanpur, Nov. 1988.

15. Glassgow, D.A., and Nelson, H.D., "Stability Analysis of Rotor-Bearing Systems Using Component Mode Synthesis", J. of Mechanical Design, Trans. of ASME, Apr. 1980, Vol. 102, pp. 352-359.

16. Lund, J.W., "Stability and Damped Critical Speeds of a Flexible Rotor in Fluid-Film Bearings", J. of Engg. for Industry, Trans. of ASME, 1974, Vol. 96, No. 2, pp. 507-517.

17. Bansal, P.N. and Kirk, R.G., "Stability and Damped Critical Speeds of Rotor-Bearing Systems", J. of Engg. for Industry, Trans. of ASME, Nov. 1975, pp. 1325-1332.

18. Prabhu, B.S., and Ramakrisihnan, K.S., "Critical Speeds, Unbalance Response and Onset of Instability of Multispan, Multi Rotor Systems", National Conference on Industrial Tribology, Hyderabad, Jul. 84.

19. Doughty, S. and Vaface, G., "Transfer Matrix Eigen Solutions for Damped Torsional Systems", J. of Engg. for Industry, Trans. of ASME, Jan. 1985, Vol. 107, pp. 128-132.

20. Tewari, Rajiv., "Sub-critical Phenomenon of Rotating Shafts due to Gravity -A Continues Approach", M. Tech. Thesis, Dept.of Mechanical Engg., I.I.T., Kanpur, 1991.

21. Gallager, R.H., "Finite Element Analysis Fundamentals", Prentice Hall, New Delhi, 1975.

22. Sastry, S.S., "Introductory Methods of Numerical Analysis", Prentice Hall, New Delhi, 1985.

23. Gupta, D.K., "Transfer Finite Element Method for Static and Dynamic Problems", M. Tech. Thesis, Dept. of Mechanical Engg., I.I.T., Kanpur, 1983.

24. Goel, S. "Critical Speeds of Rotors by Transfer Finite Element Method", M. Tech. Thesis, Dept. of Mechanical Engg., I.I.T., Kanpur, 1986.

25. Tesar, Alaxander and Fillo, Ludovit, "Transfer Matrix Method, Kluwer Academic, London, 1986.

v	Non-dimensional displacement.
V_g	Translational displacement of centre of mass along y-axis.
$\{W\}^{(ne)}$	Nodal response vector.
W_e	External work done.
β_x	Angle of shear deformation about x-axis.
β_y	Angle of shear deformation about y-axis.
ϵ	Non-dimensional mass-unbalance.
θ_x	Bending slope about x-axis.
θ_y	Bending slope about y-axis.
θ_z	Angle of rotation about s-axis.
λ	Complex natural frequency.
σ	Growth factor.
ω	Natural frequency.
ρ	Density of shaft.
ρ_o	Density of shaft at s = 0.
Ω	Non-dimensional spin speed of shaft.
Ω_o	Spin speed of shaft.
η_H	Hysteretic internal damping coefficient.
η_V	Viscous internal damping coefficient.
η_{VN}	Non-dimensional viscous internal damping coefficient.

ABSTRACT

Flexural vibrations of damped shafts including the effect of shear deformation, rotary inertia and gyroscopic action are best represented by four second order differential equations. Transfer finite element method (TFEM) has been developed in the present work for determining its critical speeds, complex natural frequencies and unbalance responses. By using four second order differential equations, all types of geometrical and natural boundary conditions, including bearing cross coupled properties can easily be incorporated exactly. This method blends the advantages of standard finite element method and transfer matrix method, i.e. solution over an element is obtained in a straight forward manner and memory requirements are considerably reduced. A variety of situations are considered and results are found to be satisfactory.

CHAPTER I

INTRODUCTION

1.1 THE PROBLEM IN BRIEF

Dynamics of rotating shafts, rotor dynamics in short is a very important area in the field of engineering as rotors are an integral part of many machines like steam and gas turbines, compressors, generators, motors etc.

It was recognised early in eighteenth century that a rotating shaft initiated vibrations of large amplitudes at certain speeds and often caused severe damage to the machinery system. The operating speedsat which this phenomenon occured came to be known as critical speeds.

A well balanced shaft also has a certain amount of unbalance which causes it to deflect from its designed position during rotation. When the shaft rotates in the deflected position, the disturbing inertia forces rotate with the shaft and shaft precesses about the bearing axis. This precesion of the shaft can be in the direction of rotation called forward precession or in the opposite direction called backward precession.

The inertia force due to unbalance has the frequency of spin speed of the shaft. Hence when the speed of precesion of shaft becomes equal to the spin speed, resonant state is reached, i.e. amplitude grows with time. When this state is reached, the corresponding spin speed of the shaft is called critical speed. Depending on the direction of precession it is called forward or backward critical speed.

1.2 LITERATURE REVIEW

The earliest work published relating to this problem was in 1869 by Rankine [1]. The operating speeds of rotating machines then were much below the first critical speed. Hence most of the work then were limited to the evaluation of first critical speed. But with advent of new technology operating speeds have become higher than the first critical speed. Consequently more recent studies treat a greater range of problems with study of effect of various system parameters on critical speeds, determination of stable range of operation etc. In 1967, Loewy and Piarulli [2] tried to illustrate the basics of rotor dynamics, in the monograph Dynamics of rotating shafts. This work treated shaft as mass less i.e. used lumped mass approach. It provided a general but qualitative information on the effects of various parameters on critical speeds and stability. This book also includes an exhaustive bibliography.

Tondl [3] in his book gives a good insight into several phenomenon of rotor dynamics. He emphasises on effect of internal

damping, unequal shaft stiffness and oil film in journal bearings. It deals comprehensively with problems concerned with the stability of rotor motion, with the creation of self excited vibrations and with nonlinear resonances. But almost the whole book is based on the assumption of mass less shaft and rigid disk. All the same the book gives an excellent review of the problems, supplemented with results of experimental investigations.

Dimentberg [4] deals with flexural transverse vibrations in his book. Major part of the book uses continuous approach. Effects of external and internal damping, dissimilarity of stiffness, multi bearing systems, uniform stiffness and non-uniform stiffness shafts with and without shear deformation effects are studied in this book. Effect of shear deformation is studied quite in detail in this text book.

Two other recent texts in this field are of Rao [5] and Goodwin [6]. These books deal with various aspects of rotor dynamics using lumped mass approach. However, the effect of rotary inertia and gyroscopic action of the disks (modelled rigid) have been considered but neglected for shafts. Another recent text is Lalanne and Ferraris [7]. This book uses continuous approach and Rayleigh Ritz finite element method. In these texts [5,6,7] the effect of shear deformation is not discussed.

An excellent collection of papers on several aspects of rotor dynamics, presented at an international symposium held at Denmark in 1974 can be found in the book edited by Niordson [8]. Another

such collection of papers are found in "Vibration and wear in high speed machinery", edited by Silvas [9].

The application of finite element method (FEM) to the problems relating to rotor dynamics was done by Ruhl and Booker [10], in 1972. They used Euler beam theory incorporating only translational kinetic energy and elastic bending theory to analyse the stability and unbalance response of a turbo rotor system. Nelson [11] improved the model by incorporating effects of rotary inertia and gyroscopic action. The effects of bearing stiffness and damping are also incorporated. Zorzi and Nelson [12], incorporated the effect of internal damping in the finite element model of [11]. The mechanism of internal damping is better represented by considering the hysteretic form rather than viscous form [4]. Reference [12] studied a model combining both the forms of damping. They also studied effect of bearing stiffnesses and damping characteristics on the instability threshold. Later in 1980, Nelson [13] used FEM, incorporating effect of shear deformation in addition to rotary inertia and gyroscopic action.

Mahendrakar [14] studied the critical speeds, natural frequencies and stability of rotating shafts by Galerkin FEM, including the effects of rotary inertia, shear deformation and gyroscopic action. He used two simultaneous second order differential equations in complex variables for undamped systems, and two simultaneous fourth order differential equations in real variables for damped systems, but with shear deformation neglected

in this. He did not study effect of bearing cross-coupled properties.

Nelson and Glassgow [15] studied natural frequencies of a shaft supported in elastic hydrodynamic bearings. They used component mode synthesis using finite element analysis, but neglecting effect of shear deformation.

A good number of authors have used transfer matrix method with lumped mass assumption. Lund [16] studied the effect of fluid film journal bearings and hysteresis internal damping on the critical speed and instability thresh hold. However, he treated the shaft as a uniform beam and neglected effect of shear deformation, rotary inertia and gyroscopic action. Bansal and Kirk [17] improved this work incorporating effect of gyroscopic moments, rotary inertia and shear deformation, and bearing characteristics. Muller's quadratic interpolation technique was employed to extract complex eigen values. Ramakrishnan and Prabhu [18] studied the unbalance response, instability and critical speeds of multispan rotor systems. Doughty and Vaface [19] studied damped torsional systems. They used Newton-Raphson method for determining complex eigen solutions.

Tewari [20] in his work has developed a continuous system approach to analyse the sub-critical phenomenon due to gravity effects in rotating shafts.

In using transfer matrix method for this kind of problems, it is difficult to obtain transfer matrices for rotors with rotary,

shear and gyroscopic effects. This difficulty is overcome easily in a very straight forward way in transfer finite element (TFEM), Gupta, Goel, Tesar and Fillo [23,24,25]. This method blends the advantages of finite element method and transfer matrix method.

Goel [24] obtained the critical speeds of uniform isotropic undamped shaft using TFEM. The effect of shear deformation, rotary inertia and gyroscopic moments were included in his analysis. In his work two second order governing differential equations solved using linear polynomial led to ill-conditioning. To avoid this two equations were combined into a single fourth order differential equation and cubic polynomials used. Although it was not possible to satisfy all the geometric and natural boundary conditions exactly in this approach, the results obtained were quite satisfactory.

1.3 AIM AND SCOPE OF PRESENT WORK

The present work aims at obtaining the critical speeds, whirling complex natural frequencies, its stability and unbalance responses of rotating shafts by developing TFEM. The governing differential equations are derived, including the effects of gyroscopic action, rotary inertia and shear deformation. These four simultaneous second order differential equations are solved using Galerkin FEM. This has the advantage of satisfying all boundary conditions, including cross-coupled bearing properties exactly. The FEM equations thus developed are transformed to

transfer finite element matrices, and complex roots obtained by Newton-Raphson method.

Studies have been done on complex natural frequencies of whirl of rotating shafts in rigid and elastic bearing supports. Hysteresis as well as viscous internal dampings have been incorporated.

Unbalance responses of a shaft-disk system are studied for different end support conditions.

CHAPTER II

FORMULATION OF GOVERNING EQUATIONS

This chapter gives the governing differential equations in non-dimensionalised form. These governing differential equations have been derived by [11,14,25], but are reproduced here for completeness sake.

2.1 SHAFT WITH NO INTERNAL DAMPING

Governing differential equations for transverse vibrations of spinning shaft, incorporating the effects of shear deformation, gyroscopic moment and rotary inertia are derived from Hamilton's principle.

Consider a differential element of length ds, as shown in Fig. (2.1). The kinetic energy of the shaft becomes [11, 14, 25], as shown in Appendix.

$$Te = \int_o^l \frac{1}{2} \rho A \, (\dot{U}^2 + \dot{V}^2) \, ds + \int_o^l \frac{1}{2} \rho I \, (\dot{\theta}_x^2 + \dot{\theta}_y^2) \, ds$$

$$+ \int_o^l \frac{1}{2} I_p \, \Omega_o^2 \, ds + \int_o^l I_p \, \Omega_o \, \dot{\theta}_x \, \theta_y \, ds \qquad (2.1.1)$$

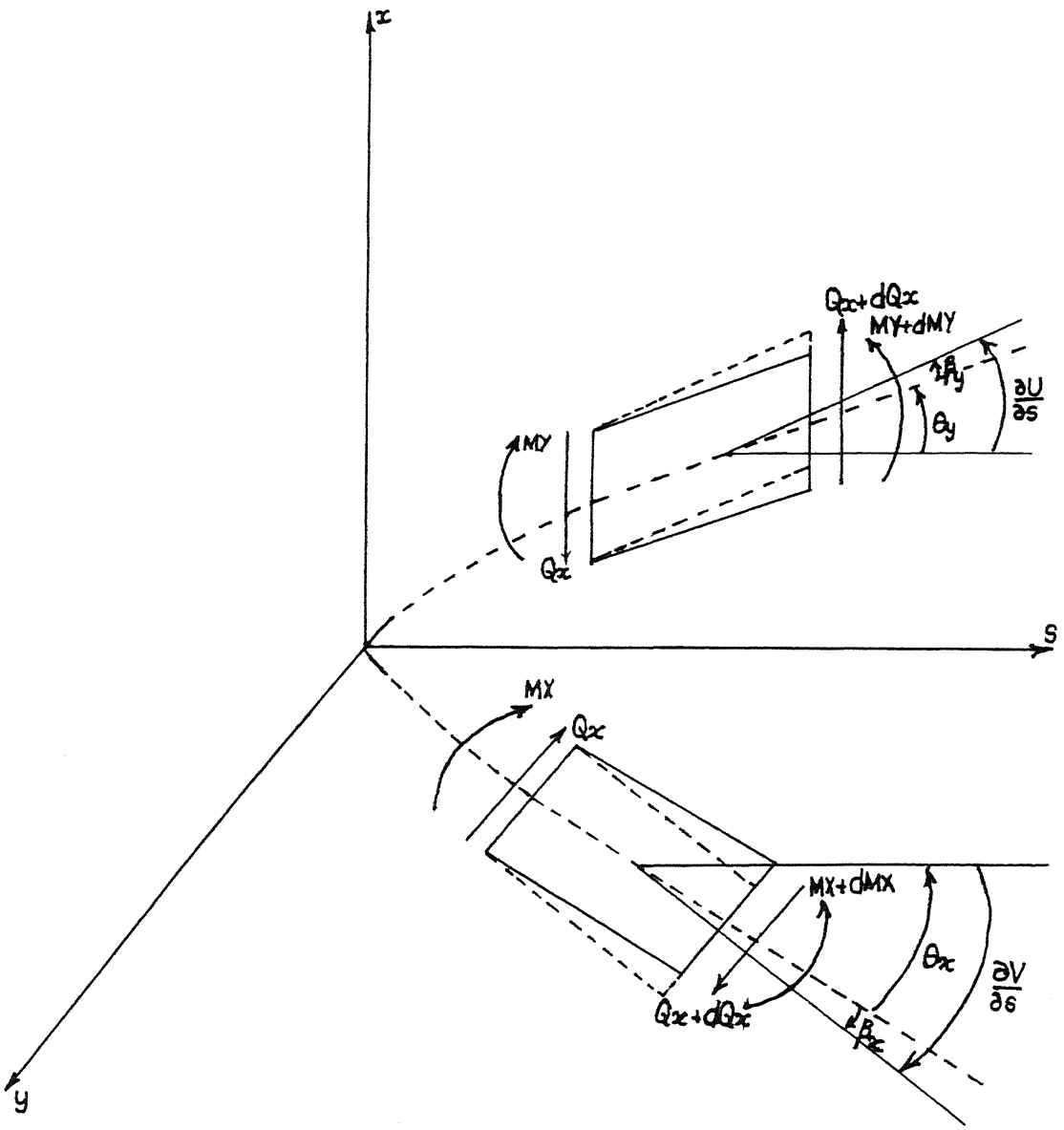

Fig. 2.1 Free-body Diagram of Differential Element in Two Planes.

Here ρA is the mass per unit length, U and V are the translations along ox and oy axes, ρI is the mass moment of inertia per unit length about the neutral axis, θ_x and θ_y are the bending slopes in ys and xs planes; I_p is the polar mass moment of inertia per unit length and Ω_o is the shaft spin speed, assumed constant. Dot represents derivatives with respect to time. In the above expression (2.1.1) first term is the energy due to translation, second term is the energy due to rotary inertia, third term is the energy due to spinning of the shaft and the last term gives the energy due to gyroscopic moments.

The strain energy of the shaft is

$$U_e = \int_o^l \frac{1}{2} EI \ (\theta_x'^2 + \theta_y'^2) \ ds + \int_o^l \frac{1}{2} k'GA \ (\beta_x^2 + \beta_y^2) \ ds \qquad (2.1.2)$$

where EI is the flexural rigidity; k' is the transverse shear form factor, a constant depending upon the shape of the cross-section, G is the shear modus, A is the area of cross section, β_y and β_x are the angles of distortion due to shear deformation about y and x axis respectively. Strokes (') represent the derivatives with respect to s. First term represents strain energy due to bending and second term strain energy due to shear deformation.

It is seen from Fig. (2.1) that the total slopes are

$$U' = \theta_y + \beta_y$$

$$V' = -\theta_x + \beta_x \qquad (2.1.3)$$

Combining eqns. (2.1.2) and (2.1.3), expression for strain energy U_e becomes,

$$U_e = \int_o^l \frac{1}{2} EI \ (\theta_x'^2 + \theta_y'^2) \ ds + \int_o^l \frac{1}{2} k'GA \left[(U' - \theta_y)^2 + (V' + \theta_x)^2 \right] ds \qquad (2.1.4)$$

The variational work done δW due to external viscous damping is

$$\delta W = \int_o^l c \dot{U} \delta U \ ds + \int_o^l c \dot{V} \delta V \ ds \qquad (2.1.5)$$

By Hamilton's principle,

$$\delta \int_{t_1}^{t_2} (Te - U_e - W) \ dt = 0$$

i.e.

$$\int_{t_1}^{t_2} \int_o^l \left\{ \frac{1}{2} \rho A \ (\dot{U}^2 + \dot{V}^2) + \frac{1}{2} \rho I \ (\dot{\theta}_x^2 + \dot{\theta}_y^2) + \frac{1}{2} I_p \ \Omega_o^2 + I_p \ \Omega_o \ \dot{\theta}_x \ \theta_y - \frac{1}{2} EI \ (\theta_x'^2 + \theta_y'^2) \ ds - \frac{1}{2} k'GA \left[(U' - \theta_y)^2 + (V' + \theta_x)^2 \right] \right\} ds \ dt - \int_{t_1}^{t_2} \int_o^l (c \dot{U} \delta U + c \dot{V} \delta V) \ ds \ dt = 0 \qquad (2.1.6)$$

Applying the δ operator and rearranging, one gets

$$\int_{t_1}^{t_2}\int_{o}^{l}\Big\{\Big[-\rho A\ddot{U} + k'GA\,(U'-\theta_y)' - c\dot{U}\Big]\,\delta U$$

$$+\Big[-\rho I\,\ddot{\theta}_y + I_p\,\Omega_o\dot{\theta}_x + (EI\theta_y')' + k'GA\,(U'-\theta_y)\Big]\,\delta\theta_y$$

$$+\Big[-\rho A\ddot{V} + k'GA\,(V'+\theta_x)' - c\dot{V}\Big]\,\delta V$$

$$+\Big[-\rho I\,\ddot{\theta}_x - I_p\Omega_o\dot{\theta}_y + (EI\theta_x')' - k'GA\,(V'+\theta_x)\Big]\,\delta\theta_x\Big\}\,ds\,dt$$

$$-EI\,\theta_x'\,\delta\theta_x\Big|_o^l - EI\,\theta_y'\,\delta\theta_y\Big|_o^l - k'GA(U'-\theta_y)\delta U\Big|_o^l$$

$$-k'GA(V'+\theta_x)\delta V\Big|_o^l = 0 \qquad (2.1.7)$$

The displacements δU, $\delta\theta_y$, δV, $\delta\theta_x$ are arbitrary, therefore

$$\rho A\ddot{U} - k'GA\,(U'-\theta_y)' + c\dot{U} = 0$$

$$\rho I\,\ddot{\theta}_y - I_p\Omega_o\dot{\theta}_x - (EI\theta_y')' - k'GA\,(U'-\theta_y) = 0 \qquad (2.1.8)$$

$$\rho A\ddot{V} - k'GA\,(V'+\theta_x)' + c\dot{V} = 0$$

$$\rho I\,\ddot{\theta}_x + I_p\Omega_o\dot{\theta}_y - (EI\theta_y')' + k'GA\,(V'+\theta_x) = 0 \qquad (2.1.9)$$

$$EI\,\theta_x'\,\delta\theta_x\Big|_o^l = 0\,,\quad k'GA(U'-\theta_y)\delta U\Big|_o^l = 0 \qquad (2.1.10)$$

$$EI\,\theta_y'\,\delta\theta_y\Big|_o^l = 0\,,\quad k'GA(V'+\theta_x)\delta V\Big|_o^l = 0 \qquad (2.1.11)$$

Equations (2.1.8) are governing differential equations in xs plane, eqns. (2.1.9) in ys plane and eqns. (2.1.10) and (2.1.11) are corresponding boundary conditions.

2.2 SHAFTS WITH INTERNAL DAMPING

References [12, 14, 16] have discussed cases of internal viscous and hysteresis damping of rotating shafts. They found that with these effects, moments MY and MX in xs and ys planes are given by

$$MY = EI\left(\frac{1+\eta_H}{\sqrt{1+\eta_H^2}}\right)\theta'_y - EI\left(\Omega_o\eta_V+\frac{\eta_H}{\sqrt{1+\eta_H^2}}\right)\theta'_x + EI\,\eta_V\,\dot{\theta}'_y$$

$$MX = EI\left(\frac{1+\eta_H}{\sqrt{1+\eta_H^2}}\right)\theta'_x + EI\left(\Omega_o\eta_V+\frac{\eta_H}{\sqrt{1+\eta_H^2}}\right)\theta'_y + EI\,\eta_V\,\dot{\theta}'_x \qquad (2.2.1)$$

where η_V is the coefficient of internal viscous damping which is frequency dependent and η_H is the loss factor, representing the frequency independent hysteretic damping.

Applying Newton's law to free-body diagram of a differential element shown in Fig. (2.1), one gets

$$\Sigma F_x = m\bar{a}_x;\ (Q_x + dQ_x) - Q_x - c\,\dot{U}\,ds = \rho A\,ds\,\ddot{U}$$

$$\Sigma M_y = I\alpha_y;\ (MY+dMY) - MY + (Q_x + dQ_x)\frac{ds}{2} + Q_x\frac{ds}{2} = \frac{d}{dt}\left(\rho I\,ds\,\dot{\theta}_y - I_p\,ds\,\Omega_o\,\theta_x\right)$$

$$\Sigma F_y = m\bar{a}_y;\ (Q_y + dQ_y) - Q_y - c\,\dot{V}\,ds = \rho A\,ds\,\ddot{V}$$

$$\Sigma M_x = I\alpha_x;\ (MX+dMX) - MX - (Q_y + dQ_y)\frac{ds}{2} - Q_y\frac{ds}{2} = \frac{d}{dt}\left(\rho I\,ds\,\dot{\theta}_x + I_p\,ds\,\Omega_o\,\theta_y\right) \qquad (2.2.2)$$

Neglecting higher order terms and rearranging, the above equations become

$$Q'_x = \rho A\ddot{U} + c\dot{U}$$

$$M'_y + Q_x = \rho I\ddot{\theta}_y - I_p\Omega_o\dot{\theta}_x$$

$$Q'_y = \rho A\ddot{V} + c\dot{V}$$

$$M'_x - Q_y = \rho I\ddot{\theta}_x + I_p\Omega_o\dot{\theta}_y \qquad (2.2.3)$$

From mechanics of solids, it is known

$$Q_x = k'GA\,(U' - \theta_y)$$

$$Q_y = k'GA\,(V' + \theta_x) \qquad (2.2.4)$$

MX and MY are defined by eqns. (2.2.1).

Combining eqns. (2.2.1), (2.2.3) and (2.2.4) and arranging one gets

$$\rho A\ddot{U} - k'GA\,(U'-\theta_y)' + c\dot{U} = 0$$

$$\rho I\,\ddot{\theta}_y - I_p\Omega_o\dot{\theta}_x - EI\left(\frac{1+\eta_H}{\sqrt{1+\eta_H^2}}\right)\theta''_y + EI\left(\Omega_o\eta_V + \frac{\eta_H}{\sqrt{1+\eta_H^2}}\right)\theta''_x$$

$$- EI\,\eta_V\,\dot{\theta}''_y - k'GA\,(U'-\theta_y) = 0 \qquad (2.2.5)$$

$$\rho A\ddot{V} - k'GA\,(V'+\theta_x)' + c\dot{V} = 0$$

$$\rho I\,\ddot{\theta}_x + I_p\Omega_o\dot{\theta}_y - EI\left(\frac{1+\eta_H}{\sqrt{1+\eta_H^2}}\right)\theta''_x - EI\left(\Omega_o\eta_V + \frac{\eta_H}{\sqrt{1+\eta_H^2}}\right)\theta''_y$$

$$- EI\,\eta_V\,\dot{\theta}''_x + k'GA\,(V'+\theta_x) = 0 \qquad (2.2.6)$$

Equations (2.2.5) and (2.2.6) are governing differential equations in xs and ys planes respectively. These are more general in nature and hence are considered from now onwards for analysis.

2.3 SHAFT WITH UNBALANCE AND NO INTERNAL DAMPING

Governing differential equations for transverse vibrations of rotating shaft, incorporating the effects of shear deformation, gyroscopic moment, rotary inertia and unbalance forces are derived from Hamilton's principle.

Consider a differential element of length ds as shown in Fig. (2.1). The geometric centre and the centre of gravity of the element do not coincide due to presence of unbalance as shown in Fig. (2.2). They are related by the equations,

$$U_g = U + e \cos \theta$$

$$V_g = V + e \sin \theta \qquad (2.3.1)$$

The kinetic energy of the shaft becomes

$$Te = \int_o^l \frac{1}{2} \rho A \, (\dot{U}_g^2 + \dot{V}_g^2) \, ds + \int_o^l \frac{1}{2} \rho I \, (\dot{\theta}_x^2 + \dot{\theta}_y^2) \, ds$$

$$+ \int_o^l \frac{1}{2} I_p \, \Omega_o^2 \, ds + \int_o^l I_p \, \Omega_o \, \dot{\theta}_x \, \theta_y \, ds \qquad (2.3.2)$$

with notations having usual meaning as discussed in section 2.1. Plugging eqn. (2.3.1) in (2.3.2) one gets,

$$Te = \frac{1}{2} \int_o^l \Big\{ \rho A \, (\dot{U}^2 + \dot{V}^2) + \rho I \, (\dot{\theta}_x^2 + \dot{\theta}_y^2)$$

$$+ I_p \, \Omega_o^2 + 2 I_p \, \Omega_o \, \dot{\theta}_x \, \theta_y - 2 \rho A \, \dot{U} \, e \sin \theta \, \dot{\theta}$$

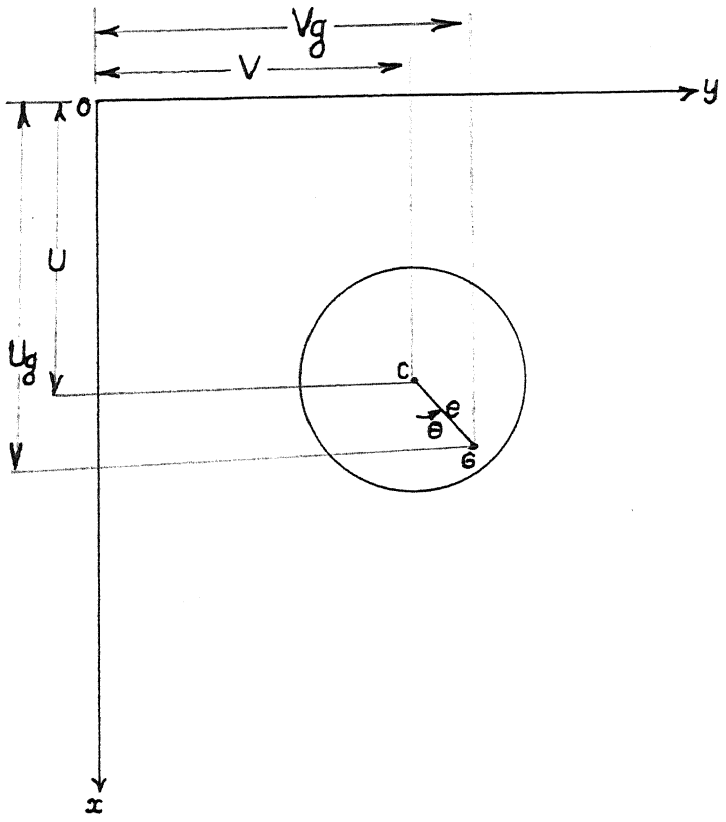

Fig. 2.2 Deflection of Centre of Mass with Unbalance.

$$+ 2\rho A\, \dot{U}\, e \cos\theta\, \dot{\theta} + e^2\, \dot{\theta}^2 \Big\}\, ds \qquad (2.3.3)$$

The strain energy U_e and variational work done δW remains as discussed in section (2.1) and is given by

$$U_e = \int_o^l \frac{1}{2} EI\, (\theta_x'^2 + \theta_y'^2)\, ds$$

$$+ \int_o^l \frac{1}{2} k'GA \left[(U' - \theta_y)^2 + (V' + \theta_x)^2 \right] ds \qquad (2.3.4)$$

$$\delta W = \int_o^l c\, \dot{U}\, \delta U\, ds + \int_o^l c\, \dot{V}\, \delta V\, ds \qquad (2.3.5)$$

By Hamilton's principle,

$$\delta \int_{t_1}^{t_2} (Te - U_e - W)\, dt = 0$$

and noting that $\dot{\theta} = \Omega_o$, the spin speed of the shaft which is a constant such that $\ddot{\theta} = 0$ one gets in the usual manner

$$\rho A\ddot{U} - k'GA\, (U'-\theta_y)' + c\dot{U} + \rho Ae\, \Omega_o^2 \cos(\Omega_o t) = 0$$

$$\rho I\, \ddot{\theta}_y - I_p \Omega_o \dot{\theta}_x - (EI\theta_y')' - k'GA\, (U'-\theta_y) = 0$$

$$\rho A\ddot{V} - k'GA\, (V'+\theta_x)' + c\dot{V} + \rho Ae\, \Omega_o^2 \sin(\Omega_o t) = 0$$

$$\rho I\, \ddot{\theta}_x + I_p \Omega_o \dot{\theta}_y - (EI\theta_y')' + k'GA\, (V'+\theta_x) = 0 \qquad (2.3.6)$$

$$EI\, \theta_x'\, \delta\theta_x \Big|_o^l = 0\,, \quad k'GA(U'-\theta_y)\delta U \Big|_o^l = 0$$

$$EI\, \theta_y'\, \delta\theta_y \Big|_o^l = 0\,, \quad k'GA(V'+\theta_x)\delta V \Big|_o^l = 0 \qquad (2.3.7)$$

Equations (2.3.6) gives governing differential equations and (2.3.7) gives the corresponding boundary conditions.

It may be noted that δ operation on ($-\rho A\ddot{U}e \sin\theta\ \dot{\theta} + \rho A\ddot{V}e \cos\theta\ \dot{\theta}$) gives terms

$$\left[\rho Ae\Omega_o^2 (\cos\theta\delta U + \sin\theta\delta V) + \rho Ae\ (\ddot{U}\sin\theta - \ddot{V}\cos\theta)\ \delta\theta \right]$$

Terms with $\delta\theta$ have been ignored in eqns. (2.3.6) as torsional vibrations have been neglected in this study.

2.4 NON-DIMENSIONALISATION

Let,

$$u = \frac{U}{L}; \qquad v = \frac{V}{L}; \qquad S = \frac{s}{L}; \qquad T = \frac{t}{T^*}$$

$$\Omega = \Omega_o T^*; \quad T^* = (\rho_o A_o L^4/E_o I_o)^{1/2}$$

$$RN = \rho/\rho_o; \quad YN = E/E_o; \quad GN = G/G_o$$

$$AN = A/A_o; \quad IN = I/I_o \qquad (2.4.1)$$

Here, L is the overall length of the shaft, ρ, E, G, A and I are density, Young's modulus, shear modulus, area and moment of inertia of the cross-section under consideration, ρ_o, E_o, G_o, A_o, I_o are properties at s = 0. Then,

$$\frac{d^nU}{ds^n} = \frac{1}{L^{n-1}}\frac{d^nu}{dS^n}; \quad \frac{d^nV}{ds^n} = \frac{1}{L^{n-1}}\frac{d^nv}{dS^n}$$

$$\frac{d^nU}{dt^n} = \frac{L}{T^{*n}}\frac{d^nu}{dT^n}; \quad \frac{d^nV}{dt^n} = \frac{L}{T^{*n}}\frac{d^nv}{dT^n};$$

$$\frac{d^n\theta_y}{ds^n} = \frac{1}{L^n}\frac{d^n\theta_y}{dS^n} \; ; \; \frac{d^n\theta_x}{ds^n} = \frac{1}{L^n}\frac{d^n\theta_x}{dS^n}$$

$$\frac{d^n\theta_y}{dt^n} = \frac{1}{T^{*n}}\frac{d^n\theta_y}{dT^n} \; ; \; \frac{d^n\theta_x}{dt^n} = \frac{1}{T^{*n}}\frac{d^n\theta_x}{dT^n} \qquad (2.4.2)$$

Plugging eqns. (2.4.1) and (2.4.2) in eqns. (2.2.5), (2.2.6) and (2.3.6) the non-dimensionalised governing equations for a differential element becomes,

$$C1\ RNM\ \ddot{u} - SN\ (u'-\theta_y)' + C1\ Dc\ \dot{u} = 0$$

$$C3\ RMN\ \ddot{\theta}_y - 2\ C3\ \Omega\ RMN\ \dot{\theta}_x - C1\ RTN\left(\frac{1+\eta_H}{\sqrt{1+\eta_H^2}}\right)\theta_y'' + C1\ RTN\left(\Omega_o\eta_{VN}+\frac{\eta_H}{\sqrt{1+\eta_H^2}}\right)\theta_x'' - C1\ RTN\ \eta_{VN}\ \dot{\theta}_y'' - SN\ (u'-\theta_y) = 0$$

$$C1\ RNM\ \ddot{v} - SN\ (v'+\theta_y)' + C1\ Dc\ \dot{u} = 0$$

$$C3\ RMN\ \ddot{\theta}_x + 2\ C3\ \Omega\ RMN\ \dot{\theta}_y - C1\ RTN\left(\frac{1+\eta_H}{\sqrt{1+\eta_H^2}}\right)\theta_x'' - C1\ RTN\left(\Omega_o\eta_{VN}+\frac{\eta_H}{\sqrt{1+\eta_H^2}}\right)\dot{\theta}_y'' - C1\ RTN\ \eta_{VN}\ \dot{\theta}_x'' + SN\ (v'+\theta_x) = 0$$

(2.4.3)

for free vibration analysis and

$$C1\ RNM\ \ddot{u} - SN\ (u'-\theta_y)' + C1\ Dc\ \dot{u} + RNM \in \Omega^2 \cos(\Omega T) = 0$$

$$C3\ RMN\ \ddot{\theta}_y - 2\ C3\ \Omega\ RMN\ \dot{\theta}_x - C1\ RTN\ \theta_y'' - SN\ (u'-\theta_y) = 0$$

$$C1\ RNM\ \ddot{v} - SN\ (v'+\theta_x)' + C1\ Dc\ \dot{u} + RNM \in \Omega^2 \sin(\Omega T) = 0$$

$$C3\ RMN\ \ddot{\theta}_x + 2\ C3\ \Omega\ RMN\ \dot{\theta}_y - C1\ RTN\ \theta_x'' + SN\ (v'+\theta_x) = 0 \qquad (2.4.4)$$

for unbalances responses, where,

$RNM = RN * AN$; $RMN = RN * IN$; $RTN = YN * IN$;

$SN = GN * AN$; $C1 = Mc\ Re^2$; $C3 = Mc\ Re^4$;

$Mc = E_o/k'\ G_o$; $Re^2 = I_o/A_o L^2$; $\eta_{VN} = \eta_V/T^*$;

$Dc = cL^4/E_o I_o T^*$; $\epsilon = C1\ (e/L)$

CHAPTER 3

TRANSFER FINITE ELEMENT FORMULATIONS

The governing differential equations for the flexural vibrations of the shaft in the non-dimensionalised form are derived and given in Chapter II by eqns (2.4.3) for free vibration analysis and (2.4.4) for unbalance responses.

3.1 FINITE ELEMENT FORMULATION FOR FREE VIBRATION ANALYSIS

The domain of the shaft length is discretised into number of finite elements as shown in Fig.(3.1). The typical finite element is shown in Fig.(3.2). The variation of u, v, θ_x and θ_y over a typical element is approximated as

$$
\begin{aligned}
u^{(e)} &= \lfloor N^u \rfloor \{u\}^{(ne)} \\
v^{(e)} &= \lfloor N^v \rfloor \{v\}^{(ne)} \\
\theta_y &= \lfloor N^{\theta_y} \rfloor \{\theta_y\}^{(ne)} \\
\theta_x &= \lfloor N^{\theta_x} \rfloor \{\theta_x\}^{(ne)}
\end{aligned}
\qquad (3.1.1)
$$

where $\lfloor N^u \rfloor$, $\lfloor N^v \rfloor$, $\lfloor N^{\theta_y} \rfloor$, $\lfloor N^{\theta_x} \rfloor$ are shape functions and $\{u\}^{(ne)}$, $\{v\}^{(ne)}$, $\{\theta_y\}^{(ne)}$ and $\{\theta_x\}^{(ne)}$ are nodal parameters.

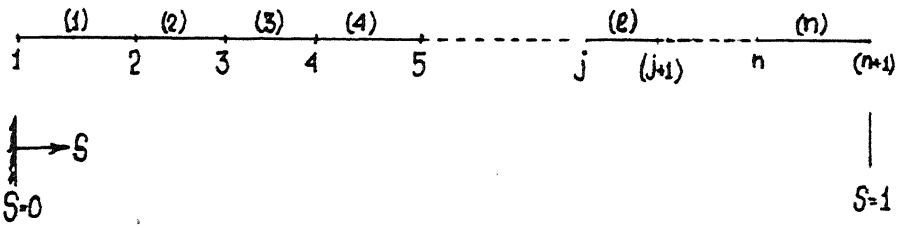

Fig. 3.1 Finite Element Discretisation of Shaft.

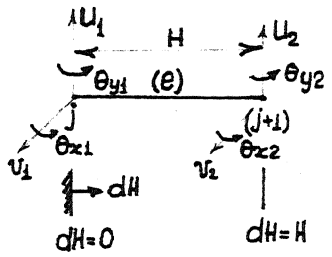

Fig. 3.2 Typical Finite Element.

Substituting eqn. (3.1.1) into eqn. (2.4.3) the residues are obtained as

$$R^{u} = C1\ RNM \int_{0}^{H} N_i^{u}\, \ddot{u}^{(e)}\, dH - SN \int_{0}^{H} N_i^{u}\, (u'^{(e)} - \theta_y^{(e)})'\, dH$$

$$+ C1\ Dc \int_{0}^{H} N_i^{u}\, \dot{u}^{(e)}\, dH$$

$$R^{v} = C1\ RNM \int_{0}^{H} N_i^{v}\, \ddot{v}^{(e)}\, dH - SN \int_{0}^{H} N_i^{v}\, (v'^{(e)} + \theta_x^{(e)})'\, dH$$

$$+ C1\ Dc \int_{0}^{H} N_i^{v}\, \dot{v}^{(e)}\, dH$$

$$R^{\theta_y} = C3\ RMN \int_{0}^{H} N_i^{\theta_y}\, \ddot{\theta}_y^{(e)}\, dH - 2\ C3\ \Omega\ RMN \int_{0}^{H} N_i^{\theta_y}\, \dot{\theta}_x^{(e)}\, dH$$

$$- C1\ RTN \int_{0}^{H} \left(\frac{1+\eta_H}{\sqrt{1+\eta_H^2}} \right) N_i^{\theta_y}\, \theta_y''^{(e)}\, dH$$

$$+ C1\ RTN \int_{0}^{H} \left(\Omega\, \eta_{VN} + \frac{\eta_H}{\sqrt{1+\eta_H^2}} \right) N_i^{\theta_y}\, \theta_x''^{(e)}\, dH$$

$$- C1\ RTN \int_{0}^{H} \eta_{VN}\, N_i^{\theta_y}\, \dot{\theta}_y''^{(e)}\, dH - SN \int_{0}^{H} N_i^{\theta_y}\, (u'^{(e)} - \theta_y^{(e)})\, dH$$

$$R^{\theta_x} = C3\ RMN \int_{0}^{H} N_i^{\theta_x}\, \ddot{\theta}_x^{(e)}\, dH + 2\ C3\ \Omega\ RMN \int_{0}^{H} N_i^{\theta_x}\, \dot{\theta}_y^{(e)}\, dH$$

$$- C1\ RTN \int_{0}^{H} \left(\frac{1+\eta_H}{\sqrt{1+\eta_H^2}} \right) N_i^{\theta_x}\, \theta_x''^{(e)}\, dH$$

$$- C1\ RTN \int_{0}^{H} \left(\Omega\, \eta_{VN} + \frac{\eta_H}{\sqrt{1+\eta_H^2}} \right) N_i^{\theta_x}\, \theta_y''^{(e)}\, dH$$

$$- C1\ RTN \int_{0}^{H} \eta_{VN}\, N_i^{\theta_x}\, \dot{\theta}_x''^{(e)}\, dH + SN \int_{0}^{H} N_i^{\theta_x}\, (v'^{(e)} + \theta_x^{(e)})\, dH$$

(3.1.2)

Minimising these residues (3.1.2) by Galerkin method, one gets after integration by parts

$$C1\ RNM \int_0^H N_i^u\ \ddot{u}^{(e)}\ dH + C1\ Dc \int_0^H N_i^u\ \dot{u}^{(e)}\ dH + SN \int_0^H N_i'^u\ u'^{(e)}\ dH$$
$$- SN \int_0^H N_i'^u\ \theta_y^{(e)}\ dH = SN\ (u'^{(e)} - \theta_y^{(e)})\ N_i^u \Big|_0^H$$

$$C1\ RNM \int_0^H N_i^v\ \ddot{v}^{(e)}\ dH + C1\ Dc \int_0^H N_i^v\ \dot{v}^{(e)}\ dH + SN \int_0^H N_i'^v\ v'^{(e)}\ dH$$
$$+ SN \int_0^H N_i'^v\ \theta_x^{(e)}\ dH = SN\ (v'^{(e)} + \theta_x^{(e)})\ N_i^v \Big|_0^H$$

$$C3\ RMN \int_0^H N_i^{\theta_y}\ \ddot{\theta}_y^{(e)}\ dH - 2\ C3\ \Omega\ RMN \int_0^H N_i^{\theta_y}\ \dot{\theta}_x^{(e)}\ dH$$
$$+ C1\ RTN \left(\frac{1+\eta_H}{\sqrt{1+\eta_H^2}} \right) \int_0^H N_i'^{\theta_y}\ \theta_y'^{(e)}\ dH$$
$$- C1\ RTN \left(\Omega\ \eta_{VN} + \frac{\eta_H}{\sqrt{1+\eta_H^2}} \right) \int_0^H N_i'^{\theta_y}\ \theta_x'^{(e)}\ dH$$
$$+ C1\ RTN \int_0^H \eta_{VN}\ N_i'^{\theta_y}\ \dot{\theta}_y'^{(e)}\ dH - SN \int_0^H N_i^{\theta_y}\ u'^{(e)}\ dH$$
$$+SN \int_0^H N_i^{\theta_y}\ \theta_y^{(e)}\ dH = \left\{ C1\ RTN \left[\left(\frac{1+\eta_H}{\sqrt{1+\eta_H^2}} \right) \theta_y'^{(e)} \right.\right.$$
$$\left.\left. - \left(\Omega\ \eta_{VN} + \frac{\eta_H}{\sqrt{1+\eta_H^2}} \right) \theta_x'^{(e)} + \eta_{VN}\ \dot{\theta}_y'^{(e)} \right] \right\} N_i^{\theta_y} \Big|_0^H$$

$$C3\ RMN \int_0^H N_i^{\theta_x}\, \ddot{\theta}_x^{(e)}\, dH + 2\ C3\ \Omega\ RMN \int_0^H N_i^{\theta_x}\, \dot{\theta}_y^{(e)}\, dH$$

$$+ C1\ RTN \left(\frac{1+\eta_H}{\sqrt{1+\eta_H^2}} \right) \int_0^H N_i'^{\theta_x}\, \theta_x'^{(e)}\, dH$$

$$+ C1\ RTN \left(\Omega\ \eta_{VN} + \frac{\eta_H}{\sqrt{1+\eta_H^2}} \right) \int_0^H N_i'^{\theta_x}\, \theta_y'^{(e)}\, dH$$

$$+ C1\ RTN\ \eta_{VN} \int_0^H N_i'^{\theta_x}\, \dot{\theta}_x'^{(e)}\, dH + SN \int_0^H N_i^{\theta_x}\, v'^{(e)}\, dH$$

$$+ SN \int_0^H N_i^{\theta_x}\, \theta_x^{(e)}\, dH = \left\{ C1\ RTN \left[\left(\frac{1+\eta_H}{\sqrt{1+\eta_H^2}} \right) \theta_x'^{(e)} \right.\right.$$

$$\left.\left. + \left(\Omega\ \eta_{VN} + \frac{\eta_H}{\sqrt{1+\eta_H^2}} \right) \theta_y'^{(e)} + \eta_{VN}\, \dot{\theta}_x'^{(e)} \right] \right\} N_i^{\theta_x} \Big|_0^H \qquad (3.1.3)$$

Study of the above shows that compatibility of u, v, θ_x and θ_y at nodes and completeness in u, v, θ_y, θ_x, u', v', θ_y' and θ_x' are required. A linear polynomial i.e. C_o elements satisfies these conditions. But these lead to ill-conditioning in these kind of problems [14,21,24]. Hence a cubic polynomial i.e. C1 elements are chosen for $u^{(e)}$, $v^{(e)}$, $\theta_y^{(e)}$ and $\theta_x^{(e)}$. The super scripts are dropped now onwards as $\lfloor N^u \rfloor = \lfloor N^v \rfloor = \lfloor N^{\theta_y} \rfloor = \lfloor N^{\theta_x} \rfloor$. Rearranging eqns. (3.1.3) in matrix form, one gets,

$$C1\ RNM \int_0^H \{N\} \lfloor N \rfloor\, dH\, \{\ddot{u}\}^{(ne)} + C1\ Dc \int_0^H \{N\} \lfloor N \rfloor\, dH\, \{\dot{u}\}^{(ne)}$$

$$+ SN \int_0^H \{N'\} \lfloor N' \rfloor\, dH\, \{u\}^{(ne)} - SN \int_0^H \{N'\} \lfloor N \rfloor\, dH\, \{\theta_y\}^{(ne)}$$

$$= SN \left(u'^{(e)} - \theta_y^{(e)} \{N\} \right|_0^H$$

$$C1\ RNM \int_0^H \{N\} \lfloor N \rfloor\ dH\ \{\ddot{v}\}^{(ne)} + C1\ Dc \int_0^H \{N\} \lfloor N \rfloor\ dH\ \{\dot{v}\}^{(ne)}$$

$$+ SN \int_0^H \{N'\} \lfloor N' \rfloor\ dH\ \{v\}^{(ne)} + SN \int_0^H \{N'\} \lfloor N \rfloor\ dH\ \{\theta_x\}^{(ne)}$$

$$= SN \left(v'^{(e)} + \theta_x^{(e)} \{N\} \right|_0^H$$

$$C3\ RMN \int_0^H \{N\} \lfloor N \rfloor\ dH\ \{\ddot{\theta}_y\}^{(ne)} - 2\ C3\ \Omega\ \ RMN \int_0^H \{N\} \lfloor N \rfloor\ dH\ \{\dot{\theta}_x\}^{(ne)}$$

$$+ C1\ RTN \left(\frac{1+\eta_H}{\sqrt{1+\eta_H^2}} \right) \int_0^H \{N'\} \lfloor N' \rfloor\ dH\ \{\theta_y\}^{(ne)}$$

$$- C1\ RTN \left(\Omega\ \eta_{VN} + \frac{\eta_H}{\sqrt{1+\eta_H^2}} \right) \int_0^H \{N'\} \lfloor N' \rfloor\ dH\ \{\theta_x\}^{(ne)}$$

$$+ C1\ RTN\ \eta_{VN} \int_0^H \{N'\} \lfloor N' \rfloor\ dH\ \{\dot{\theta}_y\}^{(ne)} - SN \int_0^H \{N\} \lfloor N' \rfloor\ dH\ \{u\}^{(ne)}$$

$$+ SN \int_0^H \{N\} \lfloor N \rfloor\ dH\ \{\theta_y\}^{(ne)}$$

$$= \left\{ C1\ RTN \left[\left(\frac{1+\eta_H}{\sqrt{1+\eta_H^2}} \right) \theta_y'^{(e)} - \left(\Omega\ \eta_{VN} + \frac{\eta_H}{\sqrt{1+\eta_H^2}} \right) \theta_x'^{(e)} \right.\right.$$

$$\left.\left. + \eta_{VN}\ \dot{\theta}_y'^{(e)} \right] \right\} \{N\} \Big|_0^H$$

$$C3\ RMN \int_0^H \{N\} \lfloor N \rfloor\ dH\ \{\ddot{\theta}_x\}^{(ne)} + 2\ C3\ \Omega\ \ RMN \int_0^H \{N\} \lfloor N \rfloor\ dH\ \{\dot{\theta}_y\}^{(ne)}$$

$$+ C1\ RTN \left(\frac{1+\eta_H}{\sqrt{1+\eta_H^2}} \right) \int_0^H \{N'\} \lfloor N' \rfloor\ dH\ \{\theta_x\}^{(ne)}$$

$$+ C1\ RTN \left(\Omega\ \eta_{VN} + \frac{\eta_H}{\sqrt{1+\eta_H^2}} \right) \int_0^H \{N'\} \lfloor N' \rfloor\ dH\ \{\theta_y\}^{(ne)}$$

$$+ C1\ RTN\ \eta_{VN} \int_0^H \{N'\} \lfloor N' \rfloor\ dH\ \{\dot{\theta}_x\}^{(ne)} + SN \int_0^H \{N\} \lfloor N' \rfloor\ dH\ \{v\}^{(ne)}$$

$$+ SN \int_0^H \{N\} \lfloor N \rfloor\ dH\ \{\theta_x\}^{(ne)}$$

$$= \left\{ C1\ RTN \left[\left(\frac{1+\eta_H}{\sqrt{1+\eta_H^2}} \right) \theta'^{(e)}_x + \left(\Omega\ \eta_{VN} + \frac{\eta_H}{\sqrt{1+\eta_H^2}} \right) \theta'^{(e)}_y + \eta_{VN}\ \dot{\theta}'^{(e)}_x \right] \right\} \{N\} \Big|_0^H \qquad (3.1.4)$$

The above equations are rearranged as

$$[M]^e \{\ddot{q}\}^{(ne)} + \left[[C]^e + [G]^e \right] \{\dot{q}\}^{(ne)} + [K]^e \{q\}^{(ne)} = \{F\}^{(ne)} \qquad (3.1.5)$$

where

$$[M]^e = \begin{bmatrix} C1\ RNM\ [A1] & [O] & [O] & [O] \\ [O] & C1\ RNM\ [A1] & [O] & [O] \\ [O] & [O] & C3\ RMN\ [A1] & [O] \\ [O] & [O] & [O] & C3\ RMN\ [1] \end{bmatrix}$$

$$[G]^e = \begin{bmatrix} [O] & [O] & [O] & [O] \\ [O] & [O] & [O] & [O] \\ [O] & [O] & [O] & -2\ C3\ \Omega\ RMN\ [A1] \\ [O] & [O] & 2\ C3\ \Omega\ RMN\ [A1] & [O] \end{bmatrix}$$

$$[C]^e = \begin{bmatrix} C1\ Dc\ [A1] & [O] & [O] & [O] \\ [O] & C1\ Dc\ [A1] & [O] & [O] \\ [O] & [O] & C1\ RTN\ \eta_{VN}\ [A2] & [O] \\ [O] & [O] & [O] & C1\ RTN\ \eta_{VN}[A2] \end{bmatrix}$$

$$K]^e =$$

$$\begin{bmatrix} SN\ [A2] & [O] & -SN\ [A3] & [O] \\ [O] & SN\ [A2] & [O] & Sn\ [A3] \\ -SN\ [A4] & [O] & C1\ RTN \left(\frac{1+\eta_H}{\sqrt{1+\eta_H^2}}\right)[A2] + SN\ [A1] & -C1\ RTN \left(\Omega\ \eta_{VN} + \frac{\eta_H}{\sqrt{1+\eta_H^2}}\right)[A2] \\ [O] & SN\ [A4] & C1\ RTN \left(\Omega\ \eta_{VN} + \frac{\eta_H}{\sqrt{1+\eta_H^2}}\right)[A2] & C1\ RTN \left(\frac{1+\eta_H}{\sqrt{1+\eta_H^2}}\right)[A2] + SN\ [A1] \end{bmatrix}$$

$$q]^{(ne)} = \lfloor \lfloor u \rfloor^{(ne)} \lfloor v \rfloor^{(ne)} \lfloor \theta_y \rfloor^{(ne)} \lfloor \theta_x \rfloor^{(ne)} \rfloor$$

$$= \lfloor u_1\ u_1'\ u_2\ u_2'\ v_1\ -v_1'\ v_2\ -v_1'\ \theta_{y1}\ \theta'_{y1}\ \theta_{y2}\ \theta'_{y2}\ \theta_{x1}\ -\theta'_{x1}\ \theta_{x2}\ -\theta'_{x2} \rfloor$$

$$F\rangle^{(ne)} = \lfloor -SU_1\ 0\ SU_2\ 0\ -SV_1\ 0\ SV_2\ 0\ -MY_1\ 0\ MY_2\ 0\ -MX_1\ 0\ MX_2\ 0 \rfloor$$

(3.1.6)

where

$$[A1] = \int_0^H \{N\} \lfloor N \rfloor \, dH$$

$$[A2] = \int_0^H \{N'\} \lfloor N' \rfloor \, dH$$

$$[A3] = \int_0^H \{N'\} \lfloor N \rfloor \, dH$$

$$[A4] = \int_0^H \{N\} \lfloor N' \rfloor \, dH$$

$$SU_1 = SN \left(u'^{(e)} - \theta_y^{(e)} \right|_1$$

$$SU_2 = SN \left(u'^{(e)} - \theta_y^{(e)} \right|_2$$

$$SV_1 = SN \left(v'^{(e)} + \theta_x^{(e)} \right|_1$$

$$SV_2 = SN \left(v'^{(e)} + \theta_x^{(e)} \right|_2$$

$$MY_1 = \left\{ C1 \; RTN \left[\left(\frac{1+\eta_H}{\sqrt{1+\eta_H^2}} \right) \theta_y'^{(e)} - \left(\Omega \, \eta_{VN} + \frac{\eta_H}{\sqrt{1+\eta_H^2}} \right) \theta_x'^{(e)} + \eta_{VN} \, \dot{\theta}_y'^{(e)} \right] \right.$$

$$MY_2 = \left\{ C1 \; RTN \left[\left(\frac{1+\eta_H}{\sqrt{1+\eta_H^2}} \right) \theta_y'^{(e)} - \left(\Omega \, \eta_{VN} + \frac{\eta_H}{\sqrt{1+\eta_H^2}} \right) \theta_x'^{(e)} + \eta_{VN} \, \dot{\theta}_y'^{(e)} \right] \right.$$

$$MX_1 = \left\{ C1 \; RTN \left[\left(\frac{1+\eta_H}{\sqrt{1+\eta_H^2}} \right) \theta_x'^{(e)} + \left(\Omega \, \eta_{VN} + \frac{\eta_H}{\sqrt{1+\eta_H^2}} \right) \theta_y'^{(e)} + \eta_{VN} \, \dot{\theta}_x'^{(e)} \right] \right.$$

$$MX_2 = \left\{ C1 \; RTN \left[\left(\frac{1+\eta_H}{\sqrt{1+\eta_H^2}} \right) \theta_x'^{(e)} + \left(\Omega \, \eta_{VN} + \frac{\eta_H}{\sqrt{1+\eta_H^2}} \right) \theta_y'^{(e)} + \eta_{VN} \, \dot{\theta}_x'^{(e)} \right] \right.$$

(3.1.7)

3.2 FINITE ELEMENT FORMULATIONS FOR UNBALANCE RESPONSES

Discretising the shaft, approximating the variations of $u^{(e)}$, $v^{(e)}$, $\theta_y^{(e)}$ and $\theta_x^{(e)}$, and applying Galerkin method to the residues obtained as discussed in the previous section, eqns. (2.4.4) that govern the unbalance response become in the matrix form as

$$[M]^e\{\ddot{q}\}^{(ne)}+\left[[C]^e+[G]^e\right]\{\dot{q}\}^{(ne)}+[K]^e\{q\}^{ne)} = \{Q\}^{(ne)}+\{F\}^{(ne)} \qquad (3.2.1)$$

where

$$[M]^e = \begin{bmatrix} C1\ RNM\ [A1] & [O] & [O] & [O] \\ [O] & C1\ RNM\ [A1] & [O] & [O] \\ [O] & [O] & C3\ RMN\ [A1] & [O] \\ [O] & [O] & [O] & C3\ RMN\ [1] \end{bmatrix}$$

$$[G]^e = \begin{bmatrix} [O] & [O] & [O] & [O] \\ [O] & [O] & [O] & [O] \\ [O] & [O] & [O] & -2\ C3\ \Omega\ RMN\ [A1] \\ [O] & [O] & 2\ C3\ \Omega\ RMN\ [A1] & [O] \end{bmatrix}$$

$$[C]^e = \begin{bmatrix} C1\ Dc\ [A1] & [O] & [O] & [O] \\ [O] & C1\ Dc\ [A1] & [O] & [O] \\ [O] & [O] & [O] & [O] \\ [O] & [O] & [O] & [O] \end{bmatrix}$$

$$[K]^e = \begin{bmatrix} SN\ [A2] & [O] & -SN\ [A3] & [O] \\ [O] & SN\ [A2] & [O] & SN\ [A3] \\ -SN\ [A4] & [O] & C1\ RTN\ [A2] + SN\ [A1] & [O] \\ [O] & SN\ [A4] & [O] & C1\ RTN\ [A2] + SN\ [A1] \end{bmatrix}$$

$$\lfloor q \rfloor^{(ne)} = \lfloor \lfloor U \rfloor^{(ne)} \lfloor V \rfloor^{(ne)} \lfloor \theta_y \rfloor^{(ne)} \lfloor \theta_x \rfloor^{(ne)} \rfloor$$

$$= \lfloor u_1\ u_1'\ u_2\ u_2'\ v_1\ -v_1'\ v_2\ -v_1'\ \theta_{y1}\ \theta_{y1}'\ \theta_{y2}\ \theta_{y2}'\ \theta_{x1}\ -\theta_{x1}'\ \theta_{x2}\ -\theta_{x2}'$$

$$\{Q\}^{(ne)} = \lfloor RMN \int_o^H \in \Omega^2 \cos \Omega T^* \lfloor N \rfloor \quad RMN \int_o^H \in \Omega^2 \sin \Omega T^* \lfloor N \rfloor \quad \lfloor O \rfloor \quad \lfloor O \rfloor \rfloor^T$$

$$\{F\}^{(ne)} = \lfloor -SU_1\ O\ SU_2\ O\ -SV_1\ O\ SV_2\ O\ -MY_1\ O\ MY_2\ O\ -MX_1\ O\ MX_2\ O\ \rfloor^T$$

(3.2.2)

where

$$[A1] = \int_O^H \{N\} \lfloor N \rfloor\ dH$$

$$[A2] = \int_O^H \{N'\} \lfloor N' \rfloor\ dH$$

$$[A3] = \int_O^H \{N'\} \lfloor N \rfloor\ dH$$

$$[A4] = \int_O^H \{N\} \lfloor N' \rfloor\ dH$$

$$SU_1 = SN\ (u'^{(e)} - \theta_y^{(e)})\big|_1$$

$$SU_2 = SN\ (u'^{(e)} - \theta_y^{(e)})\big|_2$$

$$SV_1 = SN\ (v'^{(e)} + \theta_x^{(e)})\big|_1$$

$$SV_2 = SN\ (v'^{(e)} + \theta_x^{(e)})|_2$$

$$MY_1 = C1\ RTN\ \theta'^{(e)}_y|_1$$

$$MY_2 = C1\ RTN\ \theta'^{(e)}_y|_2$$

$$MX_1 = C1\ RTN\ \theta'^{(e)}_x|_1$$

$$MX_2 = C1\ RTN\ \theta'^{(e)}_x|_2 \qquad (3.2.3)$$

3.3 FORMULATION OF FINITE ELEMENT TRANSFER MATRICES

Equations (3.1.5) represents the flexural vibrations of the beam for free vibration analysis. Eqn. (3.2.1) are the governing equations for unbalance responses of the rotating shaft. Finite element transfer matrix formulations of both cases are discussed here.

3.3.1 Free Vibration Analysis

Assuming the solution to be harmonic, the nodal displacements can be written as

$$\{q\}^{(ne)} = \{p\}^{(ne)}\ e^{\lambda T} \qquad (3.3.1)$$

where p are magnitudes and λ is the natural frequencies of whirl (both non-dimensionalized and complex) [19], as

$$p = P_R + i\ P_I$$
$$\lambda = \sigma + i\ \omega \qquad (3.3.2)$$

Here $\sqrt{P_R^2 + P_I^2}$ will give the magnitude of nodal displacement and $\tan^{-1} P_I/P_R$ represents the phase, σ is the growth factor and ω is the natural frequency of whirl. At critical speeds, the rotating shaft speed Ω is equal to ω for forward and $-\omega$ for backward whirl speeds.

Introducing eqn. (3.3.1) in eqn. (3.2.5) one gets

$$\left[\lambda^2[M]^{(e)}+\lambda\left[[G]^{(e)}+[C]^{(e)}\right]+[K]^{(e)}\right]\{p\}^{(ne)} = \{F\}^{(ne)} \qquad (3.3.3)$$

Here,

$$\{F\}^{(ne)} = \{F_R + iF_I\}^{(ne)} \qquad (3.3.4.)$$

as similar to $\{p\}$ in eqn. (3.3.2).

Substituting eqns. (3.3.2) and (3.3.4) in eqn. (3.3..3) one gets

$$\left[\left[(\sigma^2-\omega^2)\ [M] + \sigma\left[[G] + [C]\right] + [K]\right] + i\left[(2\sigma\omega)\ [M] + \omega\left[[G] + [C]\right]\right]\right]\left\{p_R + ip_I\right\} = \left\{F_R + iF_I\right\} \qquad (3.3.5)$$

Letting

$$(\sigma^2-\omega^2)\ [M] + \sigma\ [[G] + [C]] + [K] = [AR] \text{ and}$$

$$(2\sigma\omega)\ [M] + \omega\ [[G] + [C]] = [AI]$$

one gets

$$\left[\ [AR] + i\ [AI]\ \right]\left\{p_R + iP_I\right\} = \left\{F_R + iF_I\right\} \qquad (3.3.6)$$

Separating real and imaginary parts and rearranging, one gets

$$
\begin{bmatrix}
AR_{1,1} & -AI_{1,1} & AR_{1,2} & -AI_{1,2} & \cdots & AR_{1,8} & -AI_{1,8} & AR_{1,9} & -AI_{1,9} & \cdots & AR_{1,16} & -AI_{1,16} \\
AI_{1,1} & AR_{1,1} & AI_{1,2} & AR_{1,2} & \cdots & AI_{1,8} & AR_{1,8} & AI_{1,9} & AR_{1,9} & \cdots & AI_{1,16} & AR_{1,16} \\
 & & & & \cdots & & & & & \cdots & & \\
 & & & & \cdots & & & & & \cdots & & \\
 & & & & \cdots & & & & & \cdots & & \\
 & & & & \cdots & & & & & \cdots & & \\
 & & & & \cdots & & & & & \cdots & & \\
\cdots & \cdots & \cdots & \cdots & \cdots & \cdots & \cdots & \cdots & \cdots & \cdots & \cdots & \cdots \\
AR_{8,1} & -AI_{8,1} & AR_{8,2} & -AI_{8,2} & \cdots & AR_{8,8} & -AI_{8,8} & AR_{8,9} & -AI_{8,9} & \cdots & AR_{8,16} & -AI_{8,16} \\
AI_{8,1} & AR_{8,1} & AI_{8,2} & AR_{8,2} & \cdots & AI_{8,8} & AR_{8,8} & AI_{8,9} & AR_{8,9} & \cdots & AI_{8,16} & AR_{8,16} \\
AR_{9,1} & -AI_{9,1} & AR_{9,2} & -AI_{9,2} & \cdots & AR_{9,8} & -AI_{9,8} & AR_{9,9} & -AI_{9,9} & \cdots & AR_{9,16} & -AI_{9,16} \\
AI_{9,1} & AR_{9,1} & AI_{9,2} & AR_{9,2} & \cdots & AI_{9,8} & AR_{9,8} & AI_{9,9} & AR_{9,9} & \cdots & AI_{9,16} & AR_{9,16} \\
 & & & & \cdots & & & & & \cdots & & \\
 & & & & \cdots & & & & & \cdots & & \\
\cdots & \cdots & \cdots & \cdots & \cdots & \cdots & \cdots & \cdots & \cdots & \cdots & \cdots & \cdots \\
AR_{16,1} & -AI_{16,1} & AR_{16,2} & -AI_{16,2} & \cdots & AR_{16,8} & -AI_{16,8} & AR_{16,9} & -AI_{16,9} & \cdots & AR_{16,16} & -AI_{16,16} \\
AI_{16,1} & AR_{16,1} & AI_{16,2} & AR_{16,2} & \cdots & AI_{16,8} & AR_{16,8} & AI_{16,9} & AR_{16,9} & \cdots & AI_{16,16} & AR_{16,16}
\end{bmatrix}
\begin{Bmatrix}
uR_1 \\ uI_1 \\ uR'_1 \\ uI'_1 \\ uR_2 \\ uI_2 \\ \cdots \\ vR_2 \\ vI_2 \\ \theta_y R_1 \\ \theta_y I_1 \\ uR_2 \\ uI_2 \\ \cdots \\ -\theta'_x R_2 \\ -\theta'_x I_2
\end{Bmatrix}
=
\begin{Bmatrix}
-SUR_1 \\ -SUI_1 \\ 0 \\ 0 \\ SUR_2 \\ SUI_2 \\ \cdots \\ 0 \\ 0 \\ -MYR_1 \\ -MYI_1 \\ SUR_2 \\ SUI_2 \\ \cdots \\ 0 \\ 0
\end{Bmatrix}
\tag{3.3.7}
$$

Grouping the variables of node 1 and node 2 separately, the above equation can be re-written as

$$
\left[\begin{array}{cccc|ccc}
AB_{1,1} & AB_{1,2} & \cdots & AB_{1,16} & AB_{1,17} & \cdots & AB_{1,32} \\
AB_{2,1} & AB_{2,2} & \cdots & AB_{2,16} & AB_{2,17} & \cdots & AB_{1,32} \\
 & & \cdots & & & \cdots & \\
 & & \cdots & & & \cdots & \\
 & & \cdots & & & \cdots & \\
 & & \cdots & & & \cdots & \\
 & & \cdots & & & \cdots & \\
\cdots & \cdots & \cdots & \cdots & \cdots & \cdots & \cdots \\
AB_{16,1} & AB_{16,2} & \cdots & AB_{16,16} & AB_{16,17} & \cdots & AB_{16,32} \\
\hline
AB_{17,1} & AB_{17,2} & \cdots & AB_{17,16} & AB_{17,17} & \cdots & AB_{17,32} \\
 & & \cdots & & & \cdots & \\
\cdots & \cdots & \cdots & \cdots & \cdots & \cdots & \cdots \\
AB_{32,1} & AB_{32,2} & \cdots & AB_{32,16} & AB_{32,17} & \cdots & AB_{32,32}
\end{array}\right]
\left\{\begin{array}{c}
uR_1 \\ uI_1 \\ vR1 \\ vI_1 \\ \theta_y R_1 \\ \theta_y I_1 \\ \theta_x R_1 \\ \cdots \\ \theta'_x I_1 \\
\hline
uR_2 \\ uI_2 \\ \cdots \\ \theta'_x R_2
\end{array}\right\}
=
\left\{\begin{array}{c}
-SUR_1 \\ -SUI_1 \\ -SVR_1 \\ -SVI_1 \\ -MYR_1 \\ -MYI_1 \\ -MXR_1 \\ \cdots \\ 0 \\
\hline
SUR_2 \\ SUI_2 \\ \cdots \\ 0
\end{array}\right\}
\qquad (3.3.8)
$$

Equation (3.3.8) is partitioned as shown and is re-written as

$$
\begin{bmatrix}
[AB1] & [AB2] \\
16x16 & 16x16 \\
[AB3] & [AB4] \\
16x16 & 16x16
\end{bmatrix}
\begin{Bmatrix}
\{p\}_1 \\ 16x1 \\ \{p\}_2 \\ 16x1
\end{Bmatrix}
=
\begin{Bmatrix}
\{-F\}_1 \\ 16x1 \\ \{F\}_2 \\ 16x1
\end{Bmatrix}
\qquad (3.3.9)
$$

Further rearranging eqn. (3.3.9) one gets

$$\begin{Bmatrix} \{p\}_2 \\ \{F\}_2 \end{Bmatrix} = \begin{bmatrix} -[AB2]^{-1}\,[AB1] & -[AB2]^{-1} \\ [AB3]-[AB4][AB2]^{-1}[AB1] & -[AB4][AB2]^{-1} \end{bmatrix} \begin{Bmatrix} \{p\}_1 \\ \{F\}_1 \end{Bmatrix}$$

or

$$\{W\}_2 = [T]_1\ \{W\}_1 \qquad (3.3.10)$$

Here $[T]_1$ is the transfer finite element matrix relating the variables at node 2 to those at mode 1.

3.3.2 Unbalance Response Analysis

The unbalance present will induce a force given by $\epsilon\Omega^2$ so that the whirl speed becomes the spin speed of the shaft. Hence at steady state, the response will be given by

$$\{q\}^{(ne)} = \{p\}^{(ne)}\ e^{i\Omega T} \qquad (3.3.11)$$

where p are complex as discussed in the previous section, i.e.

$$p = p_R + ip_I \qquad (3.3.12)$$

Introducing eqns. (3.3.11) and (3.3.12) in eqn. (3.3.1), one gets

$$\left[-\Omega^2[M]^{(e)}+i\Omega\left[[G]^{(e)}+[C]^{(e)}\right]+[K]^{(e)}\right]\{p_R+ip_I\}^{(ne)}$$

$$= \{Q_R+iQ_I\}^{(ne)} + \{F_R+iF_I\}^{(ne)} \qquad (3.3.13)$$

Separating real and imaginary parts as discussed in Sec. (3.3.1) and re-arranging, one gets,

$$
\begin{bmatrix}
AB_{1,1} & AB_{1,2} & \cdots & AB_{1,16} & AB_{1,17} & \cdots & AB_{1,32} \\
AB_{2,1} & AB_{2,2} & \cdots & AB_{2,16} & AB_{2,17} & \cdots & AB_{1,32} \\
 & & \cdots & & & \cdots & \\
 & & \cdots & & & \cdots & \\
 & & \cdots & & & \cdots & \\
 & & \cdots & & & \cdots & \\
 & & \cdots & & & \cdots & \\
\cdots & \cdots & \cdots & \cdots & \cdots & \cdots & \cdots \\
AB_{16,1} & AB_{16,2} & \cdots & AB_{16,16} & AB_{16,17} & \cdots & AB_{16,32} \\
AB_{17,1} & AB_{17,2} & \cdots & AB_{17,16} & AB_{17,17} & \cdots & AB_{17,32} \\
 & & \cdots & & & \cdots & \\
 & & \cdots & & & \cdots & \\
\cdots & \cdots & \cdots & \cdots & \cdots & \cdots & \cdots \\
AB_{32,1} & AB_{32,2} & \cdots & AB_{32,16} & AB_{32,17} & \cdots & AB_{32,32}
\end{bmatrix}
\begin{Bmatrix}
uR_1 \\ uI_1 \\ vR_1 \\ vI_1 \\ \theta_y R_1 \\ \theta_y I_1 \\ \theta_x R_1 \\ \cdots \\ \theta'_x I_1 \\ uR_2 \\ uI_2 \\ vR_2 \\ \cdots \\ \theta'_x I_2
\end{Bmatrix}
=
\begin{Bmatrix}
Q_1 \\ 0 \\ Q_5 \\ 0 \\ 0 \\ 0 \\ 0 \\ \cdots \\ 0 \\ Q_3 \\ 0 \\ Q_5 \\ \cdots \\ 0
\end{Bmatrix}
\begin{Bmatrix}
-SUR_1 \\ -SUI_1 \\ -SVR_1 \\ -SVI_1 \\ -MYR_1 \\ -MYI_1 \\ -MXR_1 \\ \cdots \\ 0 \\ SUR_2 \\ SUI_2 \\ SVR_2 \\ \cdots \\ 0
\end{Bmatrix}
$$

(3.3.14)

Shifting the unbalance force vector into the coefficient matrix the above equation are further be rearranged as [5].

Eqn. (3.3.6) is re-arranged and obtained as :

$$
\left[\begin{array}{cccc|cccc|c}
AB_{1,1} & AB_{1,2} & \cdots & AB_{1,16} & AB_{1,17} & \cdots & AB_{1,32} & & -Q_1 \\
AB_{2,1} & AB_{2,2} & \cdots & AB_{2,16} & AB_{2,17} & \cdots & AB_{1,32} & & 0 \\
 & & \cdots & & & \cdots & & & -Q_5 \\
 & & \cdots & & & \cdots & & & 0 \\
 & & \cdots & & & \cdots & & & 0 \\
 & & \cdots & & & \cdots & & & 0 \\
 & & \cdots & & & \cdots & & & 0 \\
\cdots & \cdots & \cdots & \cdots & \cdots & \cdots & \cdots & \cdots & \cdots \\
AB_{16,1} & AB_{16,2} & \cdots & AB_{16,16} & AB_{16,17} & \cdots & AB_{16,32} & & 0 \\
\hline
AB_{17,1} & AB_{17,2} & \cdots & AB_{17,16} & AB_{17,17} & \cdots & AB_{17,32} & & -Q_3 \\
 & & \cdots & & & \cdots & & & 0 \\
 & & \cdots & & & \cdots & & & -Q_5 \\
\cdots & \cdots & \cdots & \cdots & \cdots & \cdots & \cdots & \cdots & \cdots \\
AB_{32,1} & AB_{32,2} & \cdots & AB_{32,16} & AB_{32,17} & \cdots & AB_{32,32} & & 0
\end{array}\right]
\left\{\begin{array}{c} uR_1 \\ uI_1 \\ vR_1 \\ vI_1 \\ \theta_y R_1 \\ \theta_y I_1 \\ \theta_x R_1 \\ \cdots \\ \theta'_x I_1 \\ \hline uR_2 \\ uI_2 \\ vR_2 \\ \cdots \\ \theta'_x I_2 \end{array}\right\} = \{
$$

(3.3.15)

The above equations are partitioned as shown and rewritten as

$$
\left[\begin{array}{ccc}
\underset{16\times16}{[AB1]} & \underset{16\times16}{[AB2]} & \underset{16\times1}{\{AB5\}} \\
\underset{16\times16}{[AB3]} & \underset{16\times16}{[AB4]} & \underset{16\times1}{\{AB6\}} \\
\underset{1\times16}{\lfloor 0 \rfloor} & \underset{1\times16}{\lfloor 0 \rfloor} & 1
\end{array}\right]
\left\{\begin{array}{c} \underset{16\times1}{\{p\}_1} \\ \underset{16\times1}{\{p\}_2} \\ 1 \end{array}\right\}
=
\left\{\begin{array}{c} \underset{16\times1}{\{-F\}_1} \\ \underset{16\times1}{\{F\}_2} \\ 1 \end{array}\right\}
$$

(3.3.16)

Eqn (3.36) is re-arranged and obtained as.

$$\begin{Bmatrix} \{p\}_2 \\ \{F\}_2 \\ 1 \end{Bmatrix} =$$

$$\begin{bmatrix} -[AB2]^{-1}[AB1] & -[AB2]^{-1} & -[AB2]^{-1}\{AB5\} \\ [AB3]-[AB4][AB2]^{-1}[AB1] & -[AB4][AB2]^{-1} & \{AB6\}-[AB4][AB2]^{-1}\{AB5\} \\ [0] & [0] & 1 \end{bmatrix} \begin{Bmatrix} \{p\} \\ \{F\} \\ 1 \end{Bmatrix}$$

or

$$\underset{33\times1}{\{W\}_2} = \underset{33\times33}{[T]_1} \; \underset{33\times1}{\{W\}_1} \qquad (3.3.17)$$

where $[T]_1$ is the transfer finite element matrix that relates variables at node 2 to those at node 1.

3.4 APPLYING BOUNDARY CONDITIONS

Transfer finite element matrices for each element is evaluated as discussed and multiplied over entire shaft length as

$$\{W\}_n = [T]_{n-1}\,[T]_{n-2} \ldots [T]_2\,[T]_1\,\{W\}_1 \text{ or}$$

$$\{W\}_n = [OT]\,\{W\}_1 \qquad (3.4.1)$$

where [OT] is overall transfer finite element matrix relating variables at node n to those at node 1. In eqn. (3.4.1) the nodal variables at node n and node 1 are given by

$$[W]_n = [uR_n \; uI_n \; vR_n \; vI_n \; \theta_y R_n \; \theta_y I_n \; \theta_x R_n \; \theta_x I_n \; uR'_n \; uI'_n \; vR'_n \; vI'_n \; \theta_y R'_n$$

$$\theta_y I'_n \; \theta_x R'_n \; \theta_x I'_n \; SUR_n \; SUI_n \; SVR_n \; SVI_n \; MYR_n \; MYI_n \; MXR_n \; MXI_n$$

$$0 \; 0 \; 0 \; 0 \; 0 \; 0 \; 0 \; 0]$$

$$[W]_1 = [uR_1\ uI_1\ vR_1\ vI_1\ \theta_yR_1\ \theta_yI_1\ \theta_xR_1\ \theta_xI_1\ uR_1'\ uI_1'\ vR_1'\ vI_1'\ \theta_yR_1'$$
$$\theta_yI_1'\ \theta_xR_1'\ \theta_xI_1'\ SUR_1\ SUI_1\ SVR_1\ SVI_1\ MYR_1\ MYI_1\ MXR_1\ MXI_1$$
$$0\ 0\ 0\ 0\ 0\ 0\ 0\ 0] \qquad (3.4.2)$$

Method of applying boundary conditions corresponding to a simply supported rigid bearing and elastic hydrodynamics bearings is discussed below. Other types of boundary conditions can be incorporated in a similar manner.

3.4.1 Simply Supported Rigid Bearings at Both Ends

The imaginary part of the complex variable at any node indicates the phase shift with respect to vriables at node 1. Hence the imaginary part at node 1 are all individually zeros. Hence from eqn. (3.4.2) $\{W\}_1$ reduces to

$$[W]_1 = [uR_1\ vR_1\ \theta_yR_1\ \theta_xR_1\ uR_1'\ vR_1'\ \theta_yR_1'\ \theta_xR_1'\ SUR_1\ SVR_1\ MYR_1\ MXR_1] \qquad (3.4.3)$$

For simply supported rigid bearings, the boundary conditions are

$$u_n = (uR_n + iuI_n) = v_n = (vR_n + ivI_n) = MY_n = (MYR_n + iMYI_n)$$
$$= MX_n = (MXR_n + iMXI_n) = uR_1 = vR_1 = MYR_1 = MXR_1 = 0 \qquad (3.4.4)$$

Combining eqns. (3.4.1), (3.4.2), (3.4.3) and (3.4.4) one gets

$$\underset{16\times1}{\{W\}_n} = \underset{16\times8}{[OT]}\ \underset{8\times1}{\{W\}_1} \qquad (3.4.5)$$

Here $\{W\}_n$ corresponds to vanishing variables at nodoe n and $\{W\}_1$ corresponds to nonvanishing variables at node 1, which are

$$\lfloor W \rfloor_n = \lfloor uR_n \; uI_n \; vR_n \; vI_n \; MYR_n \; MYI_n \; MXR_n \; MXI_n \; 0 \; 0 \; 0 \; 0 \; 0 \; 0 \; 0 \; 0 \rfloor$$

$$\lfloor W \rfloor_1 = \lfloor \theta_y R_1 \; \theta_x R_1 \; uR_1' \; vR_1' \; \theta_y R_1' \; \theta_x R_1' \; SUR_1 \; SVR_1 \rfloor \qquad (3.4.6)$$

Equation (3.4.6a) corresponds to a combination of real and imaginary parts of variables at node n which can be seperated into two matrices as

$$\lfloor WR \rfloor_n = \lfloor uR_n \; vR_n \; MYR_n \; MXR_n \; 0 \; 0 \; 0 \; 0 \rfloor$$

$$\lfloor WI \rfloor_n = \lfloor uI_n \; vI_n \; MYI_n \; MXI_n \; 0 \; 0 \; 0 \; 0 \rfloor \qquad (3.4.7)$$

Combining eqns. (3.4.5), (3.4.6), and (3.4.7) one gets

$$\underset{8\times1}{\{WR\}_n} = \underset{8\times8}{[OT_R]} \; \underset{8\times1}{\{W\}_1}$$

$$\underset{8\times1}{\{WI\}_n} = \underset{8\times8}{[OT_I]} \; \underset{8\times1}{\{W\}_1} \qquad (3.4.8)$$

3.4.2 Elastic Hydrodynamic Bearing Support at Both Ends

When the end supports are elastic bearings, then the boundary conditions in non-diamensionalised form become [15,17]

$$SU_1 = SN(K_{xx1}u_1 + K_{xy1}v_1 + C_{xx1}\dot{u}_1 + C_{xy1}\dot{v}_1)$$

$$SV_1 = SN(K_{yx1}u_1 + K_{yy1}v_1 + C_{yx1}\dot{u}_1 + C_{yy1}\dot{v}_1)$$

$$SU_n = -SN(K_{xxn}u_n + K_{xyn}v_n + C_{xxn}\dot{u}_n + C_{xyn}\dot{v}_n)$$

$$SV_n = -SN(K_{yxn}u_n + K_{yyn}v_n + C_{yxn}\dot{u}_n + C_{yyn}\dot{v}_n)$$

$$MY_1 = MX_1 = MY_n = MX_n = 0 \qquad (3.4.9)$$

where the bearing stiffnesses and dampings are non-diamensionalised as

$$K_{xx} = C1 \frac{k_{xx} L^3}{E_o I_o} \quad \text{and} \quad C_{xx} = C1 \frac{c_{xx} L^3}{E_o I_o T^*}$$

Assuming harmonic solution of u, v, θ_x and θ_y as

$$u = ue^{\lambda T}, \; v = ve^{\lambda T}, \; \theta_y = \theta_y e^{\lambda T}, \; \theta_x = \theta_x e^{\lambda T},$$

where $\lambda = \sigma + i\omega$ and re-arranging eqns. (3.4.9) into real and imaginary parts, one gets

$$SUR_1 = SN \left[(K_{xx1} + \sigma C_{xx1})\, uR_1 - \omega\, C_{xx1}\, uI_1 + (K_{xy1} + \sigma C_{xy1})\, vR_1 - \omega\, C_{xy1}\, vI_1 \right]$$

$$SUI_1 = SN \left[\omega\, C_{xx1}\, uR_1 + (K_{xx1} + \sigma C_{xx1})\, uI_1 + \omega\, C_{xy1}\, vR_1 + (K_{xy1} + \sigma C_{xy1})\, vI_1 \right]$$

$$SVR_1 = SN \left[(K_{yx1} + \sigma C_{yx1})\, uR_1 - \omega\, C_{yx1}\, uI_1 + (K_{yy1} + \sigma C_{yy1})\, vR_1 - \omega\, C_{yy1}\, vI_1 \right]$$

$$SVI_1 = SN \left[\omega\, C_{yx1}\, uR_1 + (K_{yx1} + \sigma C_{yx1})\, uI_1 + \omega\, C_{yy1}\, vR_1 + (K_{yy1} + \sigma C_{yy1})\, vI_1 \right]$$

$$SUR_n = SN \left[-(K_{xxn} + \sigma C_{xxn})\, uR_n + \omega\, C_{xxn}\, uI_n - (K_{xyn} + \sigma C_{xyn})\, vR_n + \omega\, C_{xyn}\, vI_n \right]$$

$$SUI_n = SN \left[-\omega\, C_{xxn}\, uR_n - (K_{xxn} + \alpha C_{xxn})\, uI_n - \omega\, C_{xyn}\, vR_n - (K_{xyn} + \alpha C_{xyn})\, vI_n \right]$$

$$SVR_n = SN \left[-(K_{yxn} + \alpha C_{yxn})\, uR_n + \omega\, C_{yxn}\, uI_n - (K_{yyn} + \alpha C_{yyn})\, vR_n + \omega\, C_{yyn}\, vI_n \right]$$

$$SVI_n = SN \left[-\omega\, C_{yxn}\, uR_n - (K_{yxn} + \alpha C_{yxn})\, uI_n - \omega\, C_{yyn}\, vR_n - (K_{yyn} + \alpha C_{yyn})\, vI_n \right]$$

$$MYR_1 = MYI_1 = MXR_1 = MXI_1 = MYR_n = MYI_n = MXR_n = MXI_n = 0 \qquad (3.4.10)$$

At both ends the nodal force variables are either zeros or a function of nodal displacements and bearing properties. Hence these can be transferred to corresponding coefficients in over all transfer matrix. It is to be noted that imaginary parts of variables at node 1 are zeros. Therefore, combining eqns. (3.4.1), (3.4.2) and (3.4.10) one gets

$$\underset{16\times 1}{\{W\}_n} = \underset{16\times 8}{[OT]}\ \underset{8\times 1}{\{W\}_1} \qquad (3.4.11)$$

Here $\{W\}_n$ corresponds to vanishing variables at node n and $\{W\}_n$ corresponds to non-vanishing variables at node 1, which are

$$\lfloor W \rfloor_n = \lfloor SUR_n\ SUI_n\ SVR_n\ SVI_n\ MYR_n\ MYI_n\ MXR_n\ MXI_n\ 0\ 0\ 0\ 0\ 0\ 0\ 0\ 0 \rfloor$$

$$\lfloor W \rfloor_1 = \lfloor uR_1\ vR_1\ \theta_y R_1\ \theta_x R_1\ uR_1'\ vR_1'\ \theta_y R_1'\ \theta_x R_1' \rfloor \qquad (3.4.12)$$

Equation (3.4.12a) can be separated into two matrices corresponding to real and imaginary parts as

$$\lfloor WR \rfloor_n = \lfloor SUR_n \; SVR_n \; MYR_n \; MXR_n \;\; 0 \; 0 \; 0 \; 0 \rfloor$$

$$\lfloor WI \rfloor_n = \lfloor SUI_n \; SVI_n \; MYI_n \; MXI_n \;\; 0 \; 0 \; 0 \; 0 \rfloor \qquad (3.4.13)$$

Combining eqns. (3.4.11), (3.4.12) and (3.4.13) one gets

$$\underset{8\times1}{\{WR\}_n} = \underset{8\times8}{[OT_R]} \; \underset{8\times1}{\{W\}_1}$$

$$\underset{8\times1}{\{WI\}_n} = \underset{8\times8}{[OT_I]} \; \underset{8\times1}{\{W\}_1} \qquad (3.4.14)$$

3.5 APPLYING BOUNDARY CONDITIONS FOR UNBALANCE RESPONSES

As discussed in Sec. (3.4), one gets over all transfer finite element matrix as

$$\underset{33\times1}{\{W\}_2} = \underset{33\times33}{[T]_1} \; \underset{33\times1}{\{W\}_1} \qquad (3.5.1)$$

This can be separated and rewritten as

$$\begin{Bmatrix} \underset{32\times1}{\{W\}_n} \\ 1 \end{Bmatrix} = \begin{bmatrix} \underset{32\times32}{[AB1]} & \underset{32\times1}{\{EF\}} \\ \underset{1\times32}{\lfloor 0 \rfloor} & 1 \end{bmatrix} \begin{Bmatrix} \underset{32\times1}{\{W\}_1} \\ 1 \end{Bmatrix} \qquad (3.5.2)$$

where $\{W\}_n$, $\{W\}_1$ are nodal variables as discussed in eqns. (3.4.2) $\{EF\}$ corresponding to the external force matrix, due to mass unbalance.

Boundary conditions are now incorporated as discussed in Sec. (3.4.1) and (3.4.2) to obtain

$$\begin{Bmatrix} \{W\}_n \\ 16\times 1 \\ 1 \end{Bmatrix} = \begin{bmatrix} [AB1] & \{EF\} \\ 16\times 8 & 16\times 1 \\ \lfloor 0 \rfloor & 1 \\ 1\times 8 & \end{bmatrix} \begin{Bmatrix} \{W\}_1 \\ 8\times 1 \\ 1 \end{Bmatrix} \qquad (3.5.3)$$

Here again $\{W\}_n$ corresponds to vanishing variables at node n and $\{W\}_n$ to non-vanishing variables at node 1. As discussed in Sec. (3.5), eqn. (3.5.3) can be separated corresponding to real and imaginary terms as

$$\underset{8\times 1}{\{WR\}_n} = \underset{8\times 8}{[OT_R]}\ \underset{8\times 1}{\{W\}_1} + \underset{8\times 1}{\{EF_R\}} = \{O\}$$

$$\underset{8\times 1}{\{WI\}_n} = \underset{8\times 8}{[OT_I]}\ \underset{8\times 1}{\{W\}_1} + \underset{8\times 1}{\{EF_I\}} = \{O\} \qquad (3.5.4)$$

CHAPTER IV

RESULTS AND DISCUSSIONS

Computer program in FORTRAN 77 have been developed to obtain natural frequencies, critical speeds and unbalance responses. Double precision was needed to obtain these results.

4.1 SOLUTION TECHNIQUES

4.1.1 Free Vibration Analysis

Assume a starting value of σ and ω (say σ_o and ω_o) and obtain eqns. (3.4.14). If assumed value of σ and ω (σ_o, ω_o) are the correct roots then

$$D1 = |OT_R| = 0$$
$$D2 = |OT_I| = 0 \qquad (4.1.1)$$

Since σ_o and ω_o are assumed values, eqns. (4.1.1) are not likely to be satisfied. Correct values of σ and ω can be obtained by using Newton-Raphson's iteration method [19,22]. Thus

$$\begin{Bmatrix} d\sigma \\ d\omega \end{Bmatrix} = \begin{bmatrix} \frac{\partial D1}{\partial \sigma} & \frac{\partial D1}{\partial \omega} \\ \frac{\partial D2}{\partial \sigma} & \frac{\partial D2}{\partial \omega} \end{bmatrix}^{-1} \begin{Bmatrix} -D1(\sigma_o,\omega_o) \\ -D2(\sigma_o,\omega_o) \end{Bmatrix} \qquad (4.1.2)$$

so that

$$\begin{Bmatrix} \sigma_1 \\ \omega_1 \end{Bmatrix} = \begin{Bmatrix} \sigma_o \\ \omega_o \end{Bmatrix} + \begin{Bmatrix} d\sigma \\ d\omega \end{Bmatrix} \qquad (4.1.3)$$

The iterative process is repeated till $d\sigma$ and $d\omega$ falls below a pre-defined small value. Derivatives in eqn. (4.1.2) are evaluated as

$$\frac{\partial D1}{\partial \sigma} = \frac{D1\ (\sigma_o+\delta\sigma, \omega_o) - D1\ (\sigma_o, \omega_o)}{\delta\sigma}$$

$$\frac{\partial D1}{\partial \omega} = \frac{D1\ (\sigma_o, \omega_o+\delta\omega) - D1\ (\sigma_o, \omega_o)}{\delta\omega}$$

$$\frac{\partial D2}{\partial \sigma} = \frac{D2\ (\sigma_o+\delta\sigma, \omega_o) - D2\ (\sigma_o, \omega_o)}{\delta\sigma}$$

$$\frac{\partial D2}{\partial \omega} = \frac{D2\ (\sigma_o, \omega_o+\delta\omega) - D2\ (\sigma_o, \omega_o)}{\delta\omega} \qquad (4.1.4)$$

Thus to evaluate these derivatives, evaluations of D1 and D2 at (σ_o, ω_o), $(\sigma_o+\delta\sigma, \omega_o)$ and $(\sigma_o, \omega_o+\delta\omega)$ are required.

In Newton-Ralphson method, convergence of the results is dependent on a good choice of starting value of σ_o and ω_o. This is a serious problem when damping either internal or external is present. Experimentation in this work has shown that this is best done, first by evaluating the undamped natural frequency. For this σ_o was assumed to be of the order of 10^{-6} and ω_o chosen arbitrarily. Now, 1% of the damping is introduced. For this, starting values of σ_o and ω_o are chosen at -2 to -3 and 90% of undamped natural frequency respectively. The roots σ and ω thus

obtained serve as the starting point for the next step of damping which was chosen at 10% whose roots were chosen to be starting value for 100% damping. The above is summarised in Table 4.1.

It was also found that $\delta\sigma$ and $\delta\omega$ at 0.1% of the present value of σ_o and ω_o gives fast converging results for this kind of problems.

4.1.2 Response Analysis

Eqns. (3.5.4) are re-written as

$$\left[OT_R\right]\left\{W\right\}_1 + \left\{EF_R\right\} = \left\{WR\right\}_n = \left\{0\right\}$$

$$\left[OT_I\right]\left\{W\right\}_1 + \left\{EF_I\right\} = \left\{WI\right\}_n = \left\{0\right\} \quad \text{or}$$

$$\left\{W\right\}_1 = -\left[OT_R\right]\left\{EF_R\right\} = -\left[OT_I\right]^{-1}\left\{EF_I\right\} \qquad (4.1.5)$$

Either of the two of the above equations can be evaluated to obtain non-vanishing variables at node 1. Both were found to give identical results as expected.

Thus, having found variables at node 1, variables at other nodes can be evaluated using eqn. (3.3.8) as

$$\{W\}_n = [T]_{n-1}\{W\}_{n-1} \qquad (4.1.6)$$

4.2 SHAFTS WITHOUT DAMPING

Critical speeds in forward precession were obtained solving eqn. (3.4.1) with all damping values taken zero for a uniform steel shaft whose material constant (Mc) is 2.9. Results were

Table 4.1: Procedural Steps for Evaluating Complex Frequencies.

Step	Damping	Starting Value		Converged Value	
		σ	ω	σ	ω
1	0	10^{-6}	arbitrary	0	ω_1
2	1%	-2 to -3	0.9 ω_1	σ_2	ω_2
3	10%	σ_2	ω_2	σ_3	ω_3
4	100%	σ_3	ω_3	σ_4 (roots)	ω_4

obtained for rotary inertia coefficient (Re) equal to 0.05 and 0.0125 which represents a shaft having length to diameter ratio 5 and 20 respectively for hinged-hinged and cantilever boundary conditions. Also results were obtained for different end conditions in two planes. 4, 6 and 8 elements were used and results are compared with [14]. These are given in Tables 2, 3 and 4; these match very well with the earlier results [14].

Reference [14] found that using 8 elements i.e. 36 degrees of freedom gave accurate results when two second order equations were used. In the present work using four second order equations, it was found 4 elements (amounting to 40 degrees of freedom) are sufficient to give accurate results with much reduced memory requirement. Hence now onwards, four elements are considered for study in this work.

4.3 SHAFTS CARRYING DISK WITHOUT DAMPING

Critical speeds are obtained for a steel shaft of 1000 mm length and 40 mm diameter with hinged-hinged supports carrying a disk of 30 mm thickness and 90 mm dia placed at 250 mm from the left end, (Fig. 4.1). The disk is also considered flexible. Effect of shaft mass to disk mass is also studied. Range of shaft mass is obtained by successively reducing the density of the shaft maintaining all other parameters constant. The results are given in Table 5. They match very well with earlier results [14].

It is seen that there is an error of 158% for a shaft to disk mass ratio of 6.584 and 30% for shaft to disk mass ratio of 0.844.

Table 4.2: Study of Critical Speeds for Hinged-Hinged. Shaft.

Re = 0.05 Mc = 2.9

Mode	No. of Elements			Mahendrakar [14] 8 Elements
	4	6	8	
1	9.6384	9.6384	9.6383	9.6383
2	35.8775	35.8775	35.8774	35.8774
3	72.1430	72.1430	72.1429	72.1429
4	112.2963	112.2960	112.2959	112.2958
5	153.2134	153.2124	153.2123	153.2122

Table 4.3: Study of Critical Speeds for Cantilever Shaft.

Re = 0.0125 Mc = 2.9

Mode	No. of Elements			Mahendrakar [14] 8 Elements
	4	6	8	
1	3.5134	3.5128	3.5123	3.5123
2	21.9454	21.9404	21.9363	21.9363
3	61.0262	61.0102	61.0101	61.01
4	118.4774	118.4604	118.4583	118.46
5	193.5804	193.5723	193.5702	193.5702

Table 4.4: Study of Critical Speeds with different support conditions in two planes

Re = 0.05 Mc = 2.9

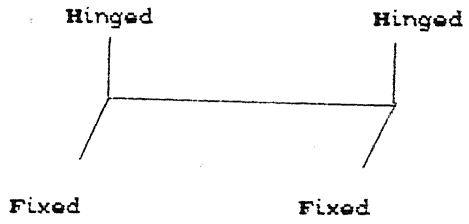

Mode	No. of Elements			Mahendrakar [14] 8 Elements
	4	6	8	
1	9.6408	9.6402	9.6383	9.6383
2	19.3448	19.3423	19.3413	19.3401
3	38.8962	35.8836	35.8800	35.8800
4	47.0583	47.0453	47.0403	47.0400
5	72.1563	72.1402	72.1483	72.1400
6	81.3672	81.3500	81.3482	81.3500

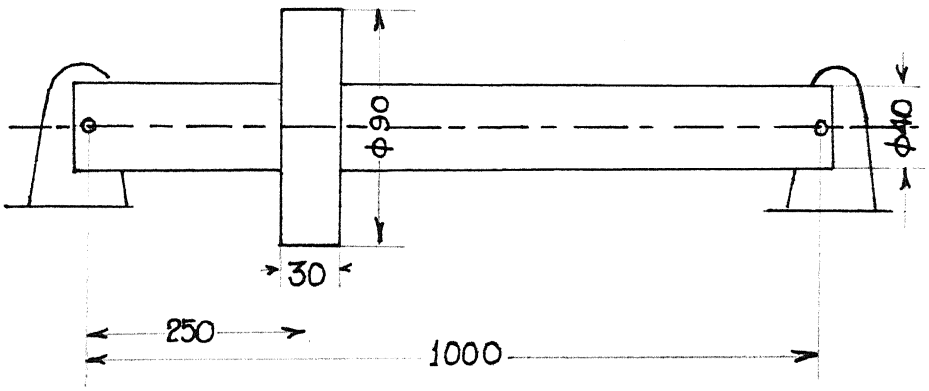

Fig 4.1 Shaft Disk System for Study of Critical Speeds.

Table 4.5: Critical speeds of shaft carrying disk.

Shaft Density	7806		4000		1000		100		10		10^{-6}	
Ratio of shaft mass to disk mass	6.584		3.374		0.844		0.084		0.0084		10^{-6}	
Modes	Present	Mahendra-kar [14]	Present	Mahendra-kar [14]	Present	Mahendra-kar [14]	Present	Mahendra-kar [14]	Present	Mahendra-kar [14]	Present	Mahendra-kar [14]
1	473.2	473.1	621.4	6211.4	940.2	940.2	1183.9	1183.9	1218.4	1218.3	1221.4	1222.2
2	1806.9	1806.9	2346.8	2346.8	3948.9	3948.9	11208.5	11208.5	37761.7	37761.7	-	-
3	4392.1	4392.1	6020.4	6020.3	11771.4	11771.4	39038.6	39038.6	122778.4	127728.2	-	-
4	8326.2	8326.1	11758.3	11758.3	24720.8	24720.8	84446.9	84446.9	269893.9	269893.9	-	-
5	12357.2	12357.2	16899.9	16899.8	33344.4	33344.4	112280.9	112280.9	360722.6	360722.6	-	-

Thus, one should not neglect the shaft mass, as error can be considerable even in first mode when shaft and disk mass are comparable.

4.4 SHAFTS WITH DAMPING AND ELASTIC BEARING SUPPORTS

To study effects of internal viscous and hysteresis damping, eqns. (3.4.1) were solved. A steel shaft with Re = 0.02 (i.e. length to diameter ratio 12.5) studied by [12, 14] with bearing supports having uncoupled stiffness and damping characteristics (i.e. $K_{xy} = K_{yx} = C_{yx} = C_{xy} = 0$) was chosen. Each case is listed below.

Case 1: Viscous damping, isotropic undamped bearings

Bearings are undamped and have isotropic bearing conditions of $K_{xx} = K_{yy} = 33.14$ (= 17.5 MN/m)

Viscous internal damping is considered with $\eta_{VN} = 0.01621$ (0.0002s). Natural frequencies and growth factor are given in Table 6, as a function of shaft spin speed Ω. The first critical speed occurs at 6.219 (4805 rpm) and second at 13.0043 (10048 rpm) in forward mode of precision. The critical speeds observed by [12, 14] were at 4980 and 10470 respectively, which are higher than the present value as [12, 14] had neglected effect of shear deformation.

The viscous internal damping begins the destabilising effect only after a certain spin speed is reached. It was found that the first mode is stable up to the first forward critical speed and instability sets in then. The second mode becomes unstable at the

Table 4.6: Natural Frequencies of Shafts with Internal Viscous Damping and Isotropic Undamped Bearings

$K_{xx} = K_{yy} = 33.14$ $C_{xx} = C_{yy} = 0.0$ $\eta_{VN} = 0.01621$

Spin Speed rpm	Growth Factor		Natural Frequency	
	Present	Nelson [12] (Non-dimensionalised)	Present	Nelson [12] (From graph and Non-dimensionalised)
(a) Forward Precession				
2000	-.1124	-.1321	6.232	6.4
	-.1102	-.1116	13.462	13.6
3000	-.0643	-	6.221	6.4
	-.0765	-	13.323	13.6
4950	.0024	.0010	6.201	6.4
	-.0327	-.0605	13.131	13.6
10000	.1428	.1303	6.172	6.4
	-.0023	-.0053	13.001	13.6
12000	.2026	.1909	6.163	6.4
	.0420	.0220	12.963	13.6
(b) Backward Precession				
2000	-.1288	-.1322	6.424	6.4
	-.1114	-.1116	13.673	13.6
3000	-.2122	-	6.462	6.4
	-.2024	-	13.683	13.6
4950	-.3137	-	6.563	6.4
	-.2983	-.1552	13.730	13.6
10000	-.3347	-.3830	6.731	6.4
	-.1785	-.1925	13.824	13.6
12000	-.3243	-.4394	6.820	6.4
	-.1988	-.2074	13.900	13.6

second critical speed. This is in agreement with observations made by [12, 14]. Both these modes remained unstable from their critical speeds upto the speed range studied.

Common observations for all the cases are listed separately after Case 5.

Case 2: Viscous damping, isotropic damped bearings

The system studied now is Case 1 with isotropic bearing dampings, $C_{xx} = C_{yy} = 0.269$ (17.5 KN.s/m). The results are shown in Table 7. The first mode is now stable up to a spin speed of 11.23 (11.6 by ref. [12,14]) and second mode up to the entire speed range studied. This matches with observations made by [12,14].

Case 3: Viscous damping, anisotropic undamped bearings

The shaft has a viscous internal damping $\eta_{VN} = 0.01621$ and is supported in two similar undamped anisotropic bearings whose stiffness are $K_{xx} = 33.14$ and $K_{yy} = 66.32$.

The results are shown in Table 8. The system is stable for the entire speed range studied which is in agreement with observations of [12, 14].

Case 4: Hysteresis damping, isotropic undamped bearings

The effect of hysteresis internal damping is studied in this case. The system is Case 1, with $\eta_{VN} = 0$ and loss factor $\eta_H = 0.0002$. Results are given in Table 9. It is seen that both forward precession modes are unstable for the entire speed range studied. Same was observed by [12, 14].

Table 4.7: Natural Frequencies of Shafts with Internal Viscous Damping and Damped Istropic Bearings

$K_{xx} = K_{yy} = 33.14 \quad C_{xx} = C_{yy} = 0.269 \quad \eta_{VN} = 0.01621$

Spin Speed rpm	Growth Factor		Natural Frequency	
	Present	Nelson [12] (Non-dimensionalised)	Present	Nelson [12] (From graph and Non-dimensionalised)
(a) Forward Precession				
2000	-.2111 -.7903	-.2329 -.7971	6.293 13.11	6.35 13.55
3000	-.1027 -.7329	- -	6.20 13.005	6.35 13.55
4950	-.0943 -.7432	-.1002 -.7662	6.185 12.897	6.35 13.55
8000	-.0322 -.6838	-.0552 -.7133	6.131 12.702	6.3 13.5
10000	.0428 -.6117	.0286 -.6746	6.108 12.543	6.2 13.45
(b) Backward Precession				
2000	-.2124 -.6913	-.2329 -.7971	6.36 13.602	6.35 13.55
3000	-.2326 -.7124	- -	6.355 13.676	6.35 13.55
4950	-.3431 -.7324	- -.7662	6.464 13.682	6.37 13.55
8000	-.3932 -.7634	-.4260 -.8680	6.625 13.743	6.4 13.6
10000	-.4343 -.7843	-.4853 -.8873	6.700 13.794	6.5 13.65

Table 4.8: Natural Frequencies of Shafts with Internal Viscous Damping and Undamped Anistropic Bearings

$K_{xx} = 33.14 \quad K_{yy} = 66.32 \quad C_{xx} = C_{yy} = 0.0 \quad \eta_{VN} = 0.01621$

Spin Speed rpm	Growth Factor		Natural Frequency	
	Present	Nelson [12] (Non-dimensionalised)	Present	Nelson [12] (From graph and Non-dimensionalised)
(a) Forward Precession				
500	-.1241	-.1318	7.423	7.6
	-.1324	-.1542	17.921	18.5
2500	-.1164	-.1297	7.420	7.6
	-.1250	-.1518	17.902	18.5
5000	-.1040	-.1226	7.416	7.6
	-.1194	-.1434	17.882	18.5
8000	-.0943	-.1114	7.384	7.6
	-.1046	-.1303	17.692	18.5
10000	-.0648	-.0960	7.301	7.6
	-.0947	-.1123	17.502	18.5
(b) Backward Precession				
500	-.2583	-.2725	6.452	6.3
	-.2128	-.2329	13.851	13.5
2500	-.2686	-.2737	6.452	6.3
	-.2177	-.2395	13.865	13.5
5000	-.2596	-.2785	6.481	6.3
	-.2104	-.2380	13.878	13.5
8000	-.2666	-.2869	6.520	6.3
	-.2244	-.2452	13.895	13.5
10000	-.2943	-.3107	6.648	6.3
	-.2565	-.2656	13.940	13.5

Table 4.9: Natural Frequencies of Shafts with Internal Hysteresis Damping and Undamped Istropic Bearings

$K_{xx} = K_{yy} = 33.14 \quad C_{xx} = C_{yy} = 0.0 \quad \eta_H = 0.0002$

Spin Speed rpm	Growth Factor		Natural Frequency	
	Present	Nelson [12] (Non-dimensionalised)	Present	Nelson [12] (From graph and Non-dimensionalised)
(a) Forward Precession				
2000	.0064 1.0724	.0018 1.0621	6.234 13.367	6.434 13.6
4000	.0065 1.0738	– –	6.234 13.352	6.434 13.6
8000	.0068 1.0754	.0018 1.0643	6.234 13.351	6.434 13.6
10000	.0071 1.0789	– –	6.235 13.324	6.4 13.6
12000	.0074 1.0813	.0018 1.0665	6.232 13.323	6.35 13.5
(b) Backward Precession				
2000	–.2353 –1.0526	–.2546 –1.0621	6.465 13.621	6.434 13.6
4000	–.2350 –1.0564	– –	6.435 13.622	6.434 13.6
8000	–.2324 –1.0602	–.2563 –1.0752	6.436 13.636	6.434 13.6
10000	–.2322 –1.0832	–	6.442 13.646	6.45 13.65
12000	–.2426 –1.0946	–.2643 –1.0852	6.446 13.656	6.50 13.7

Case 5: Hysteresis damping, isotropic damped bearings

The system studied is Case 4 with isotropic bearing dampings incorporated as $C_{xx} = C_{yy} = 0.269$. The results are shown in Table 10. Both the modes are now stable for the entire speed range studied. The observation match with those of [12;14].

In the study of above shaft with internal damping, common observations made are listed below:

(a) The natural frequencies in forward mode of precesion were found to be lower and in back ward precesion higher than those observed by [12, 14]. This is due to the effect of shear deformation which is incorporated in the present work.

(b) Forward and backward precesion frequencies were found to be very close to each other except when bearing properties were anisotropic, in which case they are wide apart.

(c) Internal viscous damping is seen to have destabilising effect beyond the first critical speed, where as internal hysteresis damping destabilises all the forward modes for the entire speed range studied.

(d) Stability of the system is improved by providing damped bearing supports. Anisotropic bearing supports also was found to increase stability.

(e) Bearing damping was found to lower the natural frequencies, as expected.

Table 4.10: Natural Frequencies of Shafts with Internal Hysteresis Dampingand Damped Istropic Bearings

$K_{xx} = K_{yy} = 33.14 \quad C_{xx} = C_{yy} = 0.269 \quad \eta_H = 0.0002$

Spin Speed rpm	Growth Factor		Natural Frequency	
	Present	Nelson [12] (Non-dimensionalised)	Present	Nelson [12] (From graph and Non-dimensionalised)
(a) Forward Precession				
2000	-.1004 -.6821	-.1006 -.6838	6.236 13.331	6.35 13.6
4000	-.1003 -.6820	- -	6.235 13.330	6.35 13.6
5000	-.1002 -.6817	-.1003 -.6836	6.234 13.288	6.35 13.5
8000	-.1006 -.6813	- -	6.223 13.247	6.30 13.4
9000	-.1012 -.6803	-.1015 -.6831	6.212 13.214	6.25 13.35
(b) Backward Precession				
2000	-.1005 -.6835	-.1006 -.6836	6.351 13.624	6.35 13.6
4000	-.1006 -.6837	- -	6.352 13.625	6.35 13.6
5000	-.1007 -.6838	-.1013 -.6843	6.352 13.626	6.35 13.6
8000	-.1007 -.6839	-	6.352 13.664	6.35 13.65
9000	-.1007 -.6839	-.1008 -.6845	6.356 13.697	6.35 13.65

4.5 SHAFT SUPPORTED IN ELASTIC HYDRODYNAMIC BEARINGS WITH CROSS COUPLING

A steel shaft with following properties supported at both ends in similar hydrodynamic bearings is studied for natural frequencies over a range of shaft spin speeds. This shaft was also studied by [15,17].

Shaft density	7833 kg/m^3
Young's modulus	206.8 GPa
Shaft diameter	101.6 mm
Shaft length	1270.0 mm
Bearing L/D ratio	0.25, 0.5

For bearing with L/D ratio as 0.5, the bearing properties were obtained from the polynomial functions given by [5]. When the L/D ratio was 0.25, direct values were not available and were extrapolated from graphs for L/D ratios of 0.5 and 1.0 given by [5].

Results for bearing with L/D ratio of 0.5 are given in Table 11 and compared with those given by [15], obtained by FEM. The present frequencies are slightly lower than those of [15] as shear deformations have been accounted for in the present work.

Results for bearings with L/D ratio of 0.25 are given in Table 12 and compared with those given by [17], using transfer matrix method with lumped mass approach. Present frequencies are higher than those of [17]. This is expected to a large extent as

Table 4.11: Natural Frequencies of Shaft Supported in Elastic Hydrodynamic Bearing (L/D = 0.5)

Bearing Properties: Length = 50.8 mm
Diameter = 101.6 mm
Radial Clearance = .0508 mm
Viscosity of Oil = 6.9 Centipoise

Spin Speed rpm	Growth Factor		Natural Frequency	
	Present	Glassgow [15] (Non-dimensionalised)	Present	Glassgow [15] (Non-dimensionalised)
2000	-1.4343	-1.6809	1.3208	1.5508
	-1.6384	–	1.1684	–
	-2.2432	–	9.6856	–
	- .8643	–	9.4324	–
4000	-1.9325	-2.1215	3.2623	3.5642
	-2.3264	–	3.0646	–
	-2.6864	–	9.7356	–
	- .9852	–	9.5358	–
6000	- .9367	-1.0590	5.0175	5.2809
	-2.4643	–	4.8964	–
	-2.9384	–	9.8863	–
	-1.6987	–	9.6634	–
8000	- .1678	- .2398	5.5639	5.8406
	-2.8324	–	5.0634	–
	-3.6047	–	9.9264	–
	-1.9964	–	9.8643	–
10000	.2736	.2632	6.0043	6.1243
	-2.6364	–	5.6746	–
	-3.8243	–	9.9986	–
	-2.3246	–	9.8885	–
12000	.6829	.6553	6.2059	6.4235
	-2.6046	–	5.7623	–
	-4.0246	–	10.6432	–
	-2.5648	–	9.9893	–

Table 4.12: Natural Frequencies of Shaft Supported in Elastic Hydrodynamic Bearing (L/D = 0.25)

Bearing Properties: Length = 25.4 mm
Diameter = 101.6 mm
Radial Clearance = .0508 mm
Viscosity of Oil = 6.9 Centipoise

Spin Speed rpm	Growth Factor		Natural Frequency	
	Present	Bansal [17] (Non-dimensionalised)	Present	Bansal [17] (Non-dimensionalised)
2000	-2.2855	-1.5205	2.0129	1.6190
	-2.0156	-1.5105	2.2270	1.7333
	-3.0343	-2.1321	11.5220	9.6309
	- .6326	- .4561	10.6343	9.9175
3000	-2.3434	-1.8102	2.3449	2.3155
	-2.1032	-1.7308	3.0726	2.5493
	-3.3667	-2.4656	10.7360	9.4927
	- .9643	- .6317	9.9725	9.8732
4000	-2.7436	-1.9507	3.0343	2.9996
	-1.6343	-1.7272	3.9641	3.3568
	-3.8563	-2.7302	10.3241	9.3996
	-1.0432	- .7595	9.4487	9.8398
6000	-2.8667	-2.0568	5.4321	4.3601
	-1.4634	-1.2242	6.0343	4.8314
	-4.1123	-3.5790	10.4321	9.4011
	-1.4836	- .9243	9.9642	9.8398
7000	-2.8734	-2.0484	6.2147	5.0395
	-1.4343	-1.2241	6.9923	5.3711
	-4.6321	-4.0720	10.8843	9.6076
	-1.6800	- .9594	9.9144	9.7855
8000	-2.6324	-1.9806	6.6762	5.7057
	- .9343	- .4164	7.7324	5.7500
	-4.7343	-4.5850	11.4323	9.9718
	-1.7243	- .9754	9.8836	9.7435
9000	-2.2343	-1.8992	7.0173	6.3712
	- .2367	- .0781	7.4361	6.0605
	-4.8434	-4.8410	11.8843	10.3920
	-1.9643	-	9.7323	-

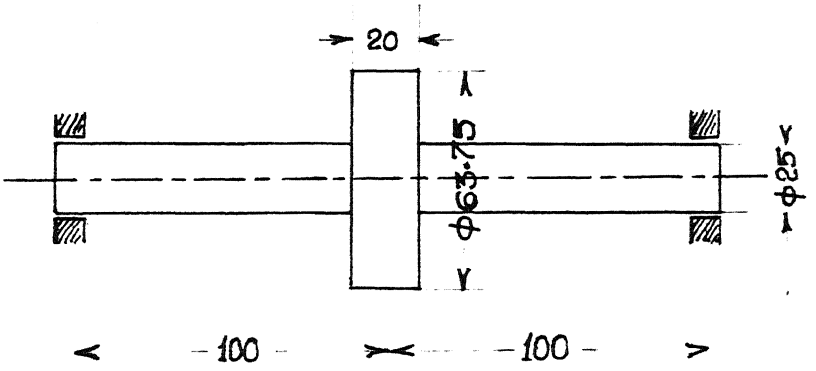

Fig. 4.2 Shaft Disk System with Unbalance.

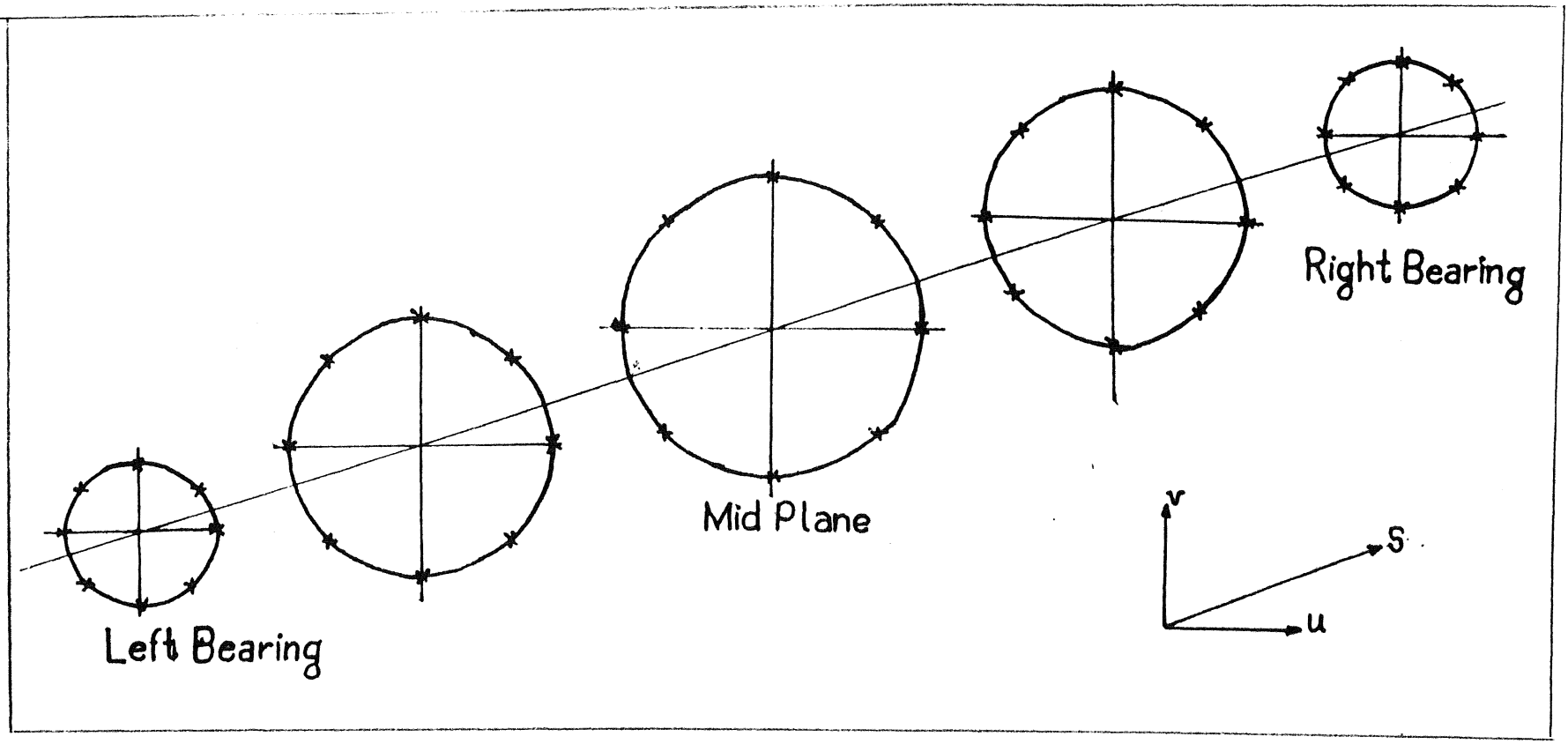

FIG 4·4 Whirl Orbit At 6000 rpm (Case 1)

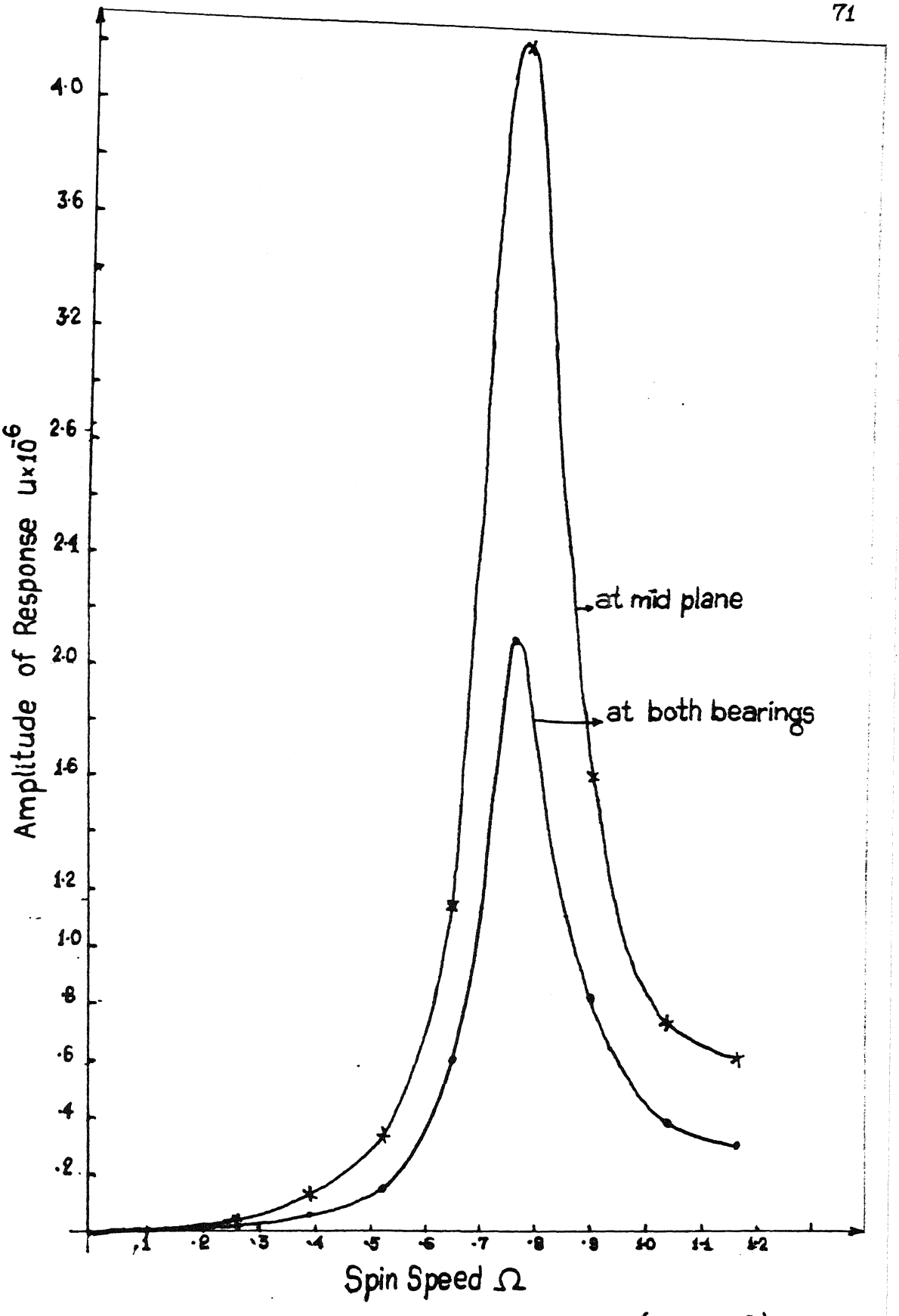

Fig 4·5 Amplitude Vs Spin Speed (Case 2)

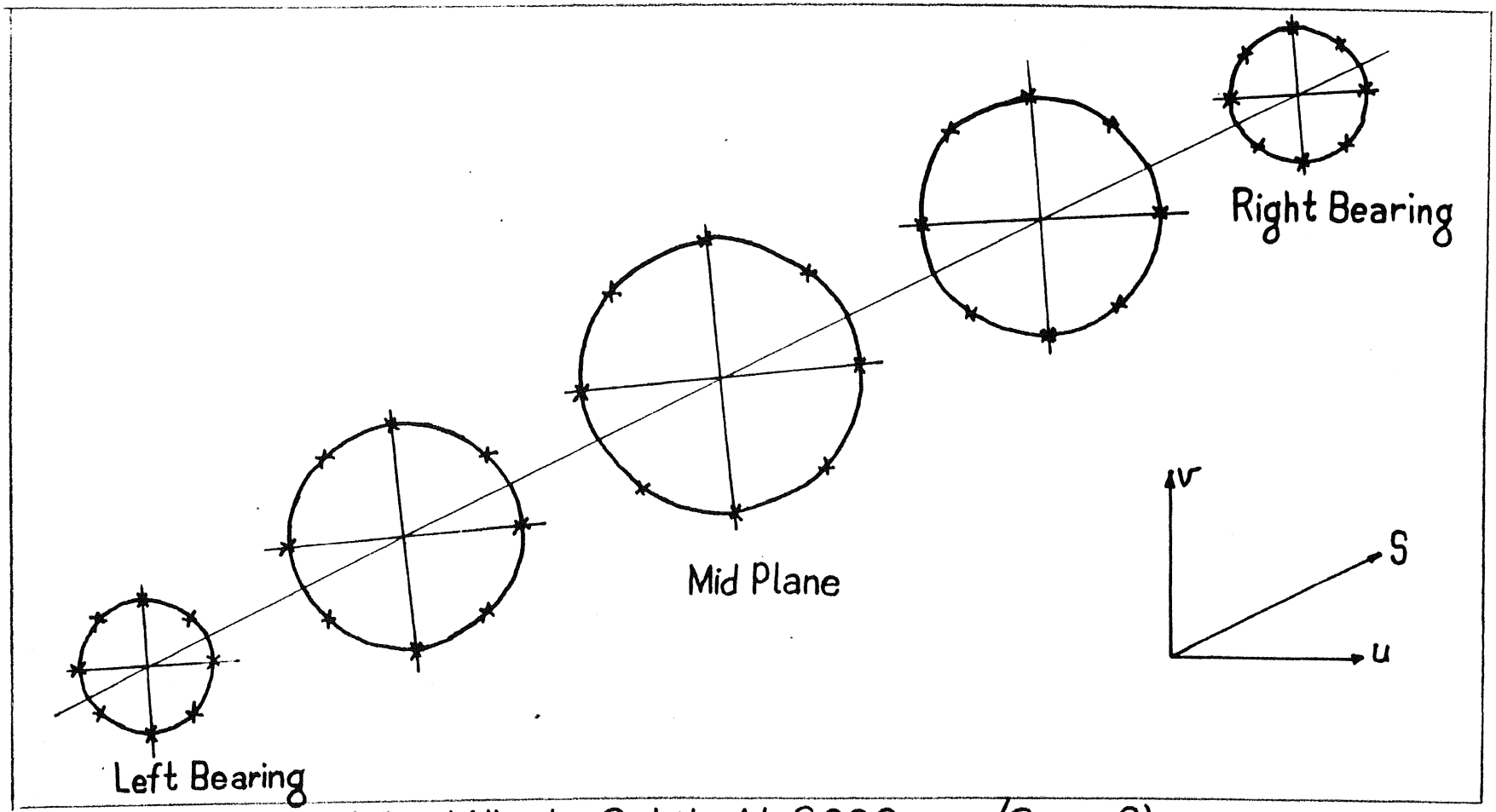

Fig 4.6 Whirl Orbit At 6000rpm (Case 2)

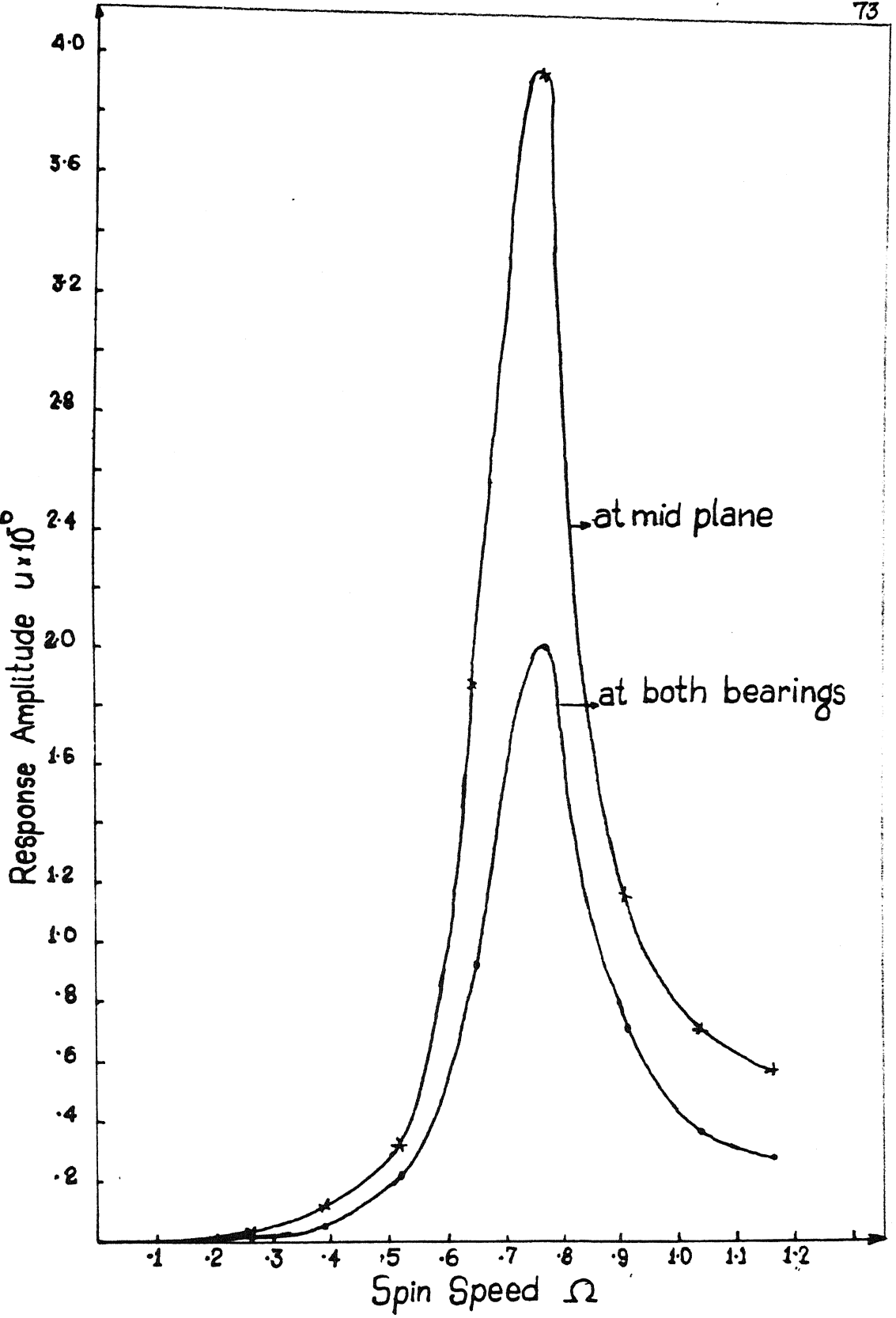

Fig. 4.7 Amplitude Vs Spin Speed (Case 3)

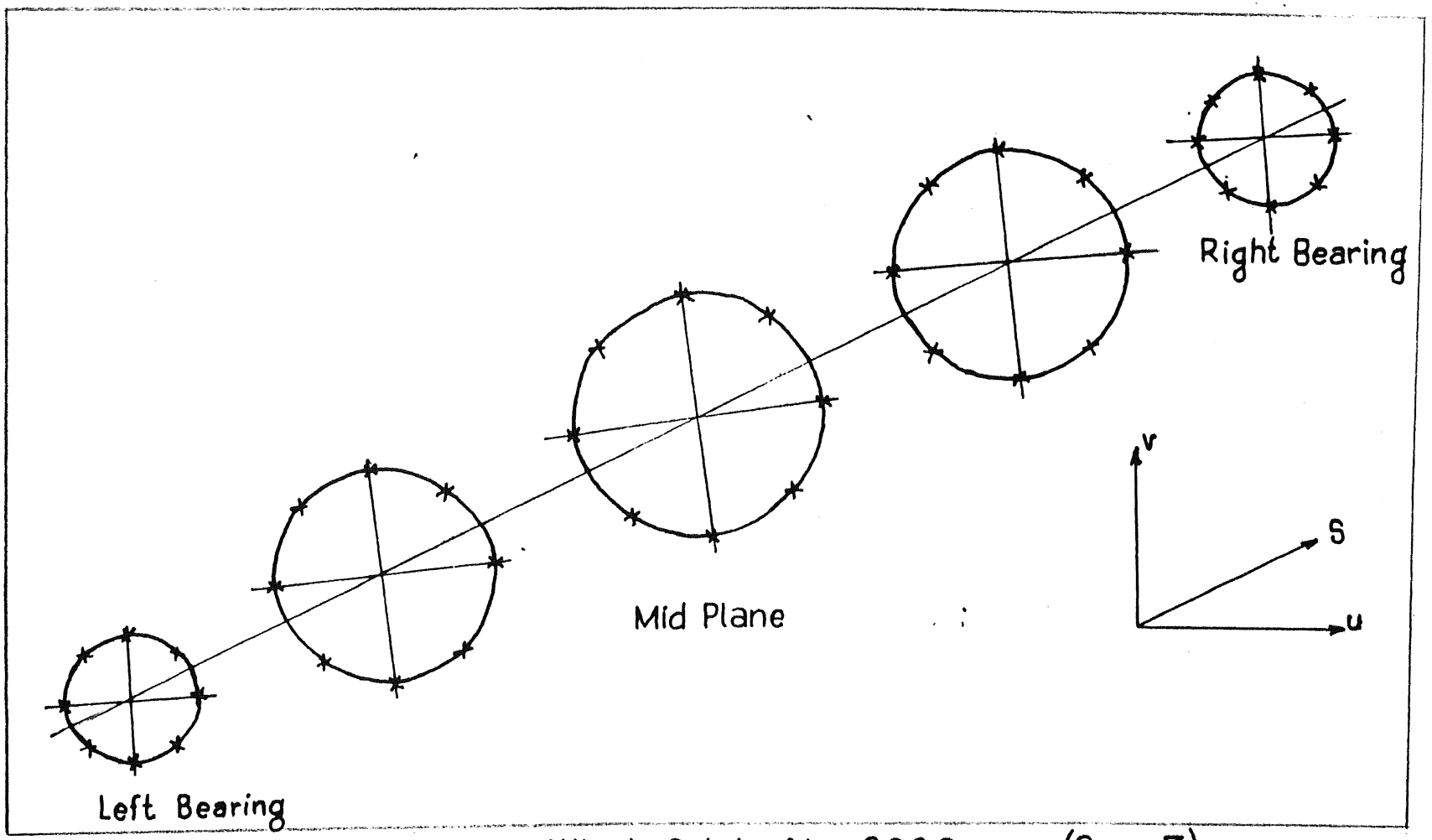

Fig 4·8 Whirl Orbit At 6000 rpm (Case 3)

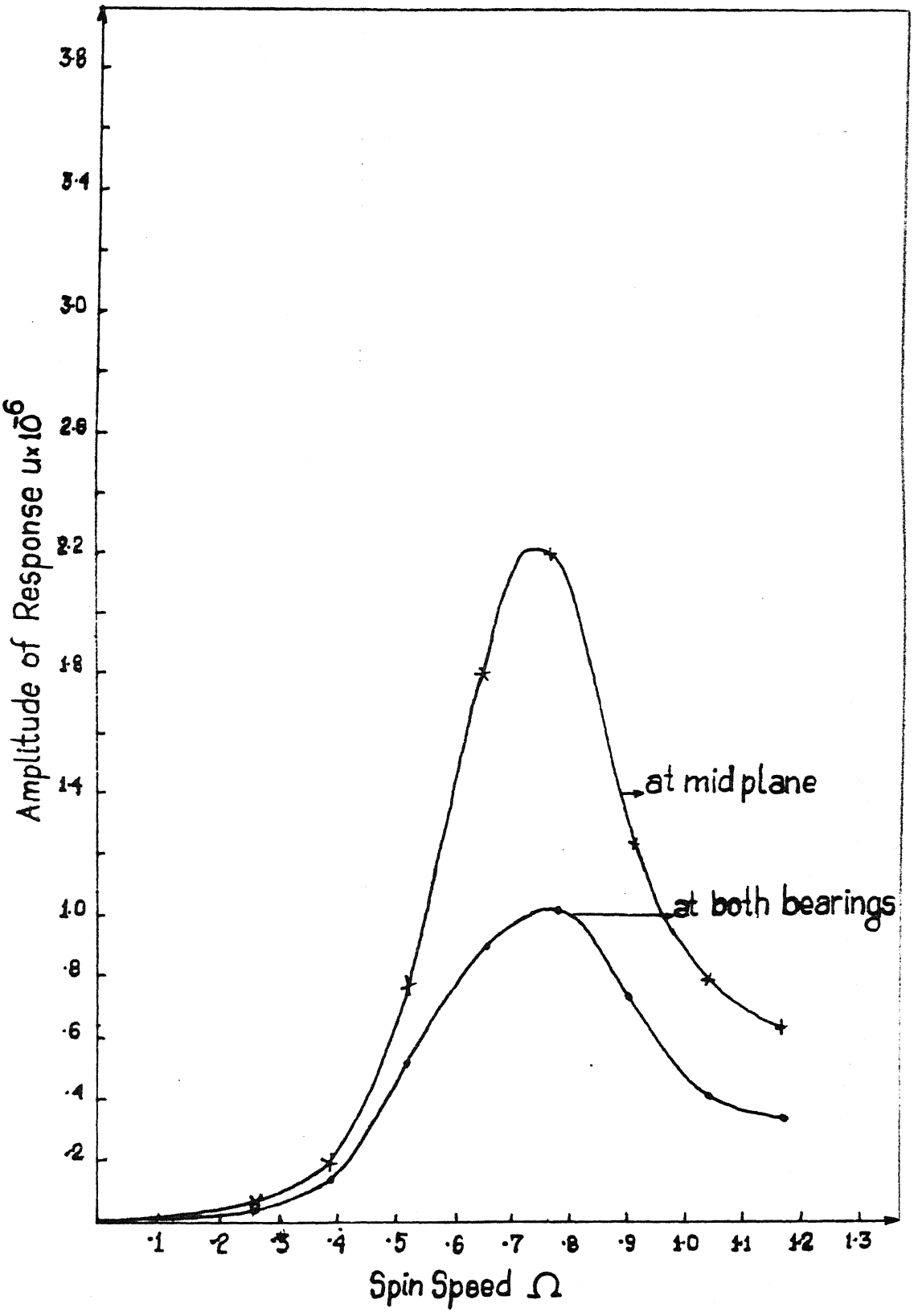

Fig 4·9 Amplitude Vs Spin Speed (Case 4)

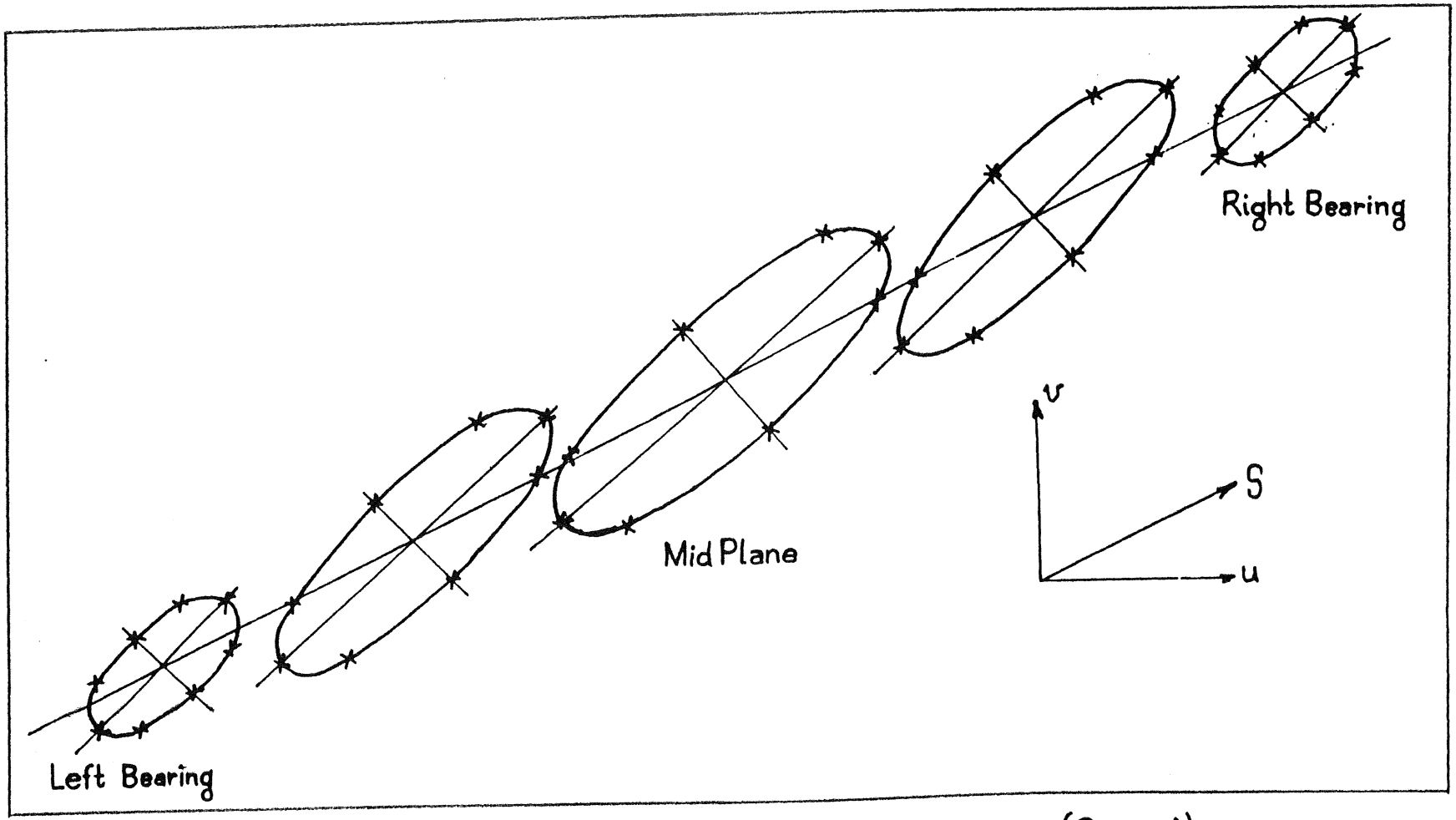

Fig. 4·10 Whirl Orbit At 6000 rpm (Case 4)

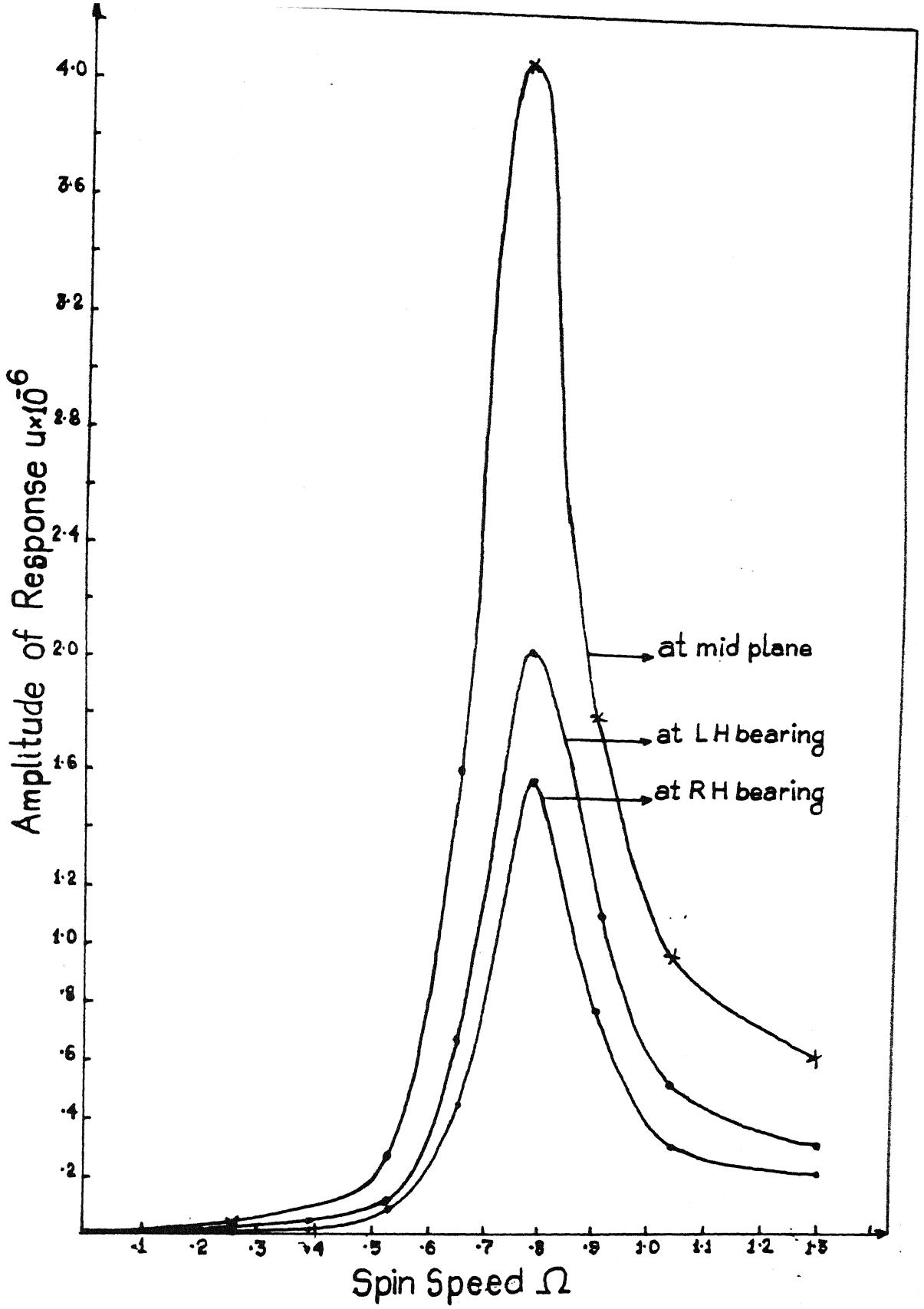

Fig. 4·11 Amplitude Vs Spin Speed (Case 5)

CHAPTER V

CONCLUSIONS

The following conclusions emerge from the present work:

1) Transfer finite element method is easily applicable for study of flexural vibrations of rotating shops. Results obtained with fewer elements are quite accurate.

2) By using four second order differential equations, all types of geometrical and natural boundary conditions,including bearing cross coupled properties can easily be incorporated exactly.

3) When shear deformation is considered, results obtained using cubic polynomials approximation are very accurate with no ill conditioning.

4) Neglecting shaft mass can lead large errors. The mass of the shaft is taken care of in a routine way in the present work.

5) Effect of shear deformation was found to lower natural frequencies in forward whirl and increase in backward whirl.

6) Internal viscous damping begins destabilising effect after a certain spin speed is reached. Hysteretic internal damping has destabilising effect at all speed.

7) Damped bearing supports increases system stability. Anisotropic bearing are also found to improve stability.

8) For unbalanced shaft system with damping, there is a phase shift of response along axial length.

9) The whirl orbit for isotropic bearings are circular, while for anisotropic bearings they are elliptical, as expected.

APPENDIX

DERIVATION OF KINETIC ENERGY

The shaft cross section has a rotation θ_x about x-axis, θ_y about y-axis, θ_z about s-axis, translation U along x-axis and V along y-axis as mentioned in section (2.1). The kinetic energy due to rotation is obtained as follows:

Consider a frame of reference abc attached to shaft cross section such that c-axis is normal to the cross section, a,b axes are in the plane of cross section and mutually perpendicular to each other and c-axis. Then the rotations of cross sections, relative to xys frame are also the rotations of frame abc relative to xys. Initially the axes of abc frame are considered to be coincident with xys frame. The final position of frame, abc relative to xys is determined by the following sequence of rotations:

1) A rotation by θ_x about x-axis gives $a_2b_2c_2$ (Fig. A-1a)
2) A rotation by θ_y about b_2-axis gives $a_1b_1c_1$ (Fig. A-1b)
3) A rotation by θ_z about c_1-axis gives a b c (Fig. A-1c)

Referring to Fig. (A-1a), the position of $a_2b_2c_2$ frame after the rotation of θ_x relative to xys frame as

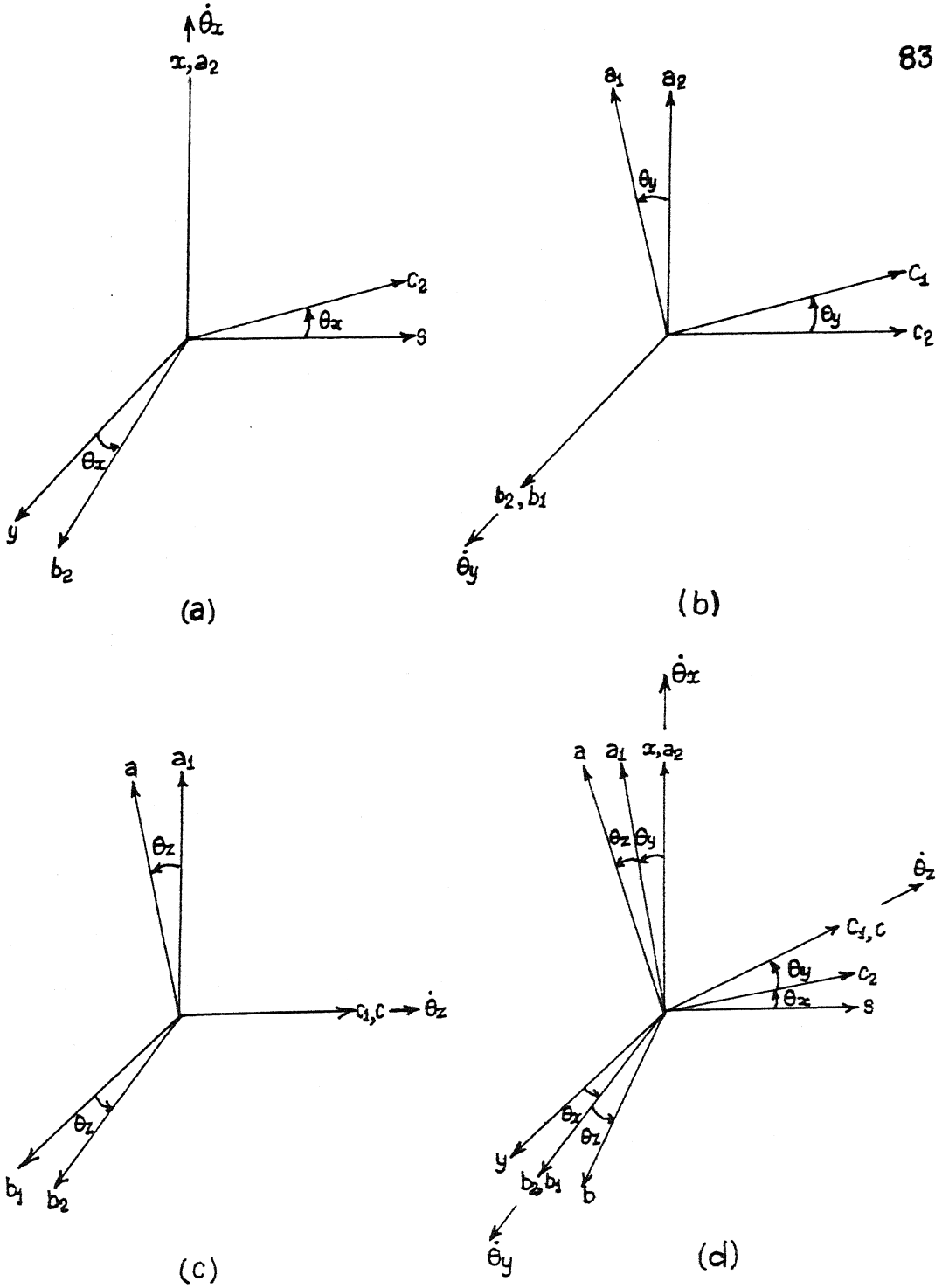

A-1 (a) Rotation θ_x about x-axis.

(b) Rotation θ_y about b2-axis.

(c) Rotation θ_z about c1-axis.

(d) Final Position of abc Frame.

$$\begin{Bmatrix} a_2 \\ b_2 \\ c_2 \end{Bmatrix} = \begin{bmatrix} 1 & 0 & 0 \\ 0 & \cos\theta_z & \sin\theta_z \\ 0 & -\sin\theta_z & \cos\theta_z \end{bmatrix} \begin{Bmatrix} x \\ y \\ s \end{Bmatrix} \qquad \text{(A-1.1)}$$

Similarly, the position of frame $a_1b_1c_1$ relative to $a_2b_2c_2$ after the rotation θ_y is, Fig.(A-1b).

$$\begin{Bmatrix} a_1 \\ b_1 \\ c_1 \end{Bmatrix} = \begin{bmatrix} \cos\theta_y & 0 & -\sin\theta_y \\ 0 & 1 & 0 \\ \sin\theta_y & 0 & \cos\theta_y \end{bmatrix} \begin{Bmatrix} a_2 \\ b_2 \\ c_2 \end{Bmatrix} \qquad \text{(A-1.2)}$$

Finally, the position of frame abc relative to frame $a_1b_1c_1$ after the rotation θ_z is, Fig. (A-1c).

$$\begin{Bmatrix} a \\ b \\ c \end{Bmatrix} = \begin{bmatrix} \cos\theta_z & \sin\theta_z & 0 \\ -\sin\theta_z & \cos\theta_z & 0 \\ 0 & 0 & 1 \end{bmatrix} \begin{Bmatrix} a_1 \\ b_1 \\ c_1 \end{Bmatrix} \qquad \text{(A-1.3)}$$

The final position of abc after the above rotations is shown in Fig. (A-1d). The frame abc, has the angular velocities $\dot{\theta}_x$ along a_2, $\dot{\theta}_y$ along b_1 and $\dot{\theta}_z$ along c. The component of $\dot{\theta}_x$ along the directions a,b and c can be obtained by the following transformations using eqns. (A-1.2) and (A-1.3) as

$$\begin{Bmatrix} \dot{\theta}_x,a \\ \dot{\theta}_x,b \\ \dot{\theta}_x,c \end{Bmatrix} = \begin{bmatrix} \cos\theta_z & \sin\theta_z & 0 \\ -\sin\theta_z & \cos\theta_z & 0 \\ 0 & 0 & 1 \end{bmatrix} \begin{bmatrix} \cos\theta_y & 0 & -\sin\theta_y \\ 0 & 1 & 0 \\ \sin\theta_y & 0 & \cos\theta_y \end{bmatrix} \begin{Bmatrix} \dot{\theta}_x \\ 0 \\ 0 \end{Bmatrix}$$

$$= \begin{Bmatrix} \cos\theta_z \cos\theta_y \dot{\theta}_x \\ -\cos\theta_y \sin\theta_z \dot{\theta}_x \\ \sin\theta_z \dot{\theta}_x \end{Bmatrix} \qquad \text{(A-1.4)}$$

Similarly the components of $\dot{\theta}_y$ along the directions a,b and c are obtained using eqn. (A-1.3) as

$$\begin{Bmatrix} \dot{\theta}_y,a \\ \dot{\theta}_y,b \\ \dot{\theta}_y,c \end{Bmatrix} = \begin{bmatrix} \cos\theta_z & \sin\theta_z & 0 \\ -\sin\theta_z & \cos\theta_z & 0 \\ 0 & 0 & 1 \end{bmatrix} \begin{Bmatrix} 0 \\ \dot{\theta}_y \\ 0 \end{Bmatrix} = \begin{Bmatrix} \sin\theta_z\,\dot{\theta}_y \\ \cos\theta_z\,\dot{\theta}_y \\ 0 \end{Bmatrix} \qquad \text{(A-1.5)}$$

The angular velocity vector $\dot{\theta}_z$ is along c direction, thus no transformation is required. Hence the angular velocities along a, b and c directions, due to the rotations θ_x, θ_y and θ_z are obtained using eqns (A-1.4) and (A-1.5) as

$$\begin{aligned} \Omega_a &= \dot{\theta}_x,a + \dot{\theta}_y,a + \dot{\theta}_z,a = \dot{\theta}_x \cos\theta_z \cos\theta_y + \dot{\theta}_y \sin\theta_z \\ \Omega_b &= \dot{\theta}_x,b + \dot{\theta}_y,b + \dot{\theta}_z,b = -\dot{\theta}_x \cos\theta_y \sin\theta_z + \dot{\theta}_y \cos\theta_z \\ \Omega_c &= \dot{\theta}_x,c + \dot{\theta}_y,c + \dot{\theta}_z,c = \dot{\theta}_x \sin\theta_y + \dot{\theta}_z \end{aligned} \qquad \text{(A-1.6)}$$

As the directions a,b and c are also the principle directions, the kinetic energy due to translation and rotation becomes,

$$Te = \frac{1}{2}\int_o^l \left[\rho A(\dot{U}^2+\dot{V}^2) + \rho I(\Omega_a^2+\Omega_b^2) + I_p\Omega_c^2\right] ds \qquad \text{(A-1.7)}$$

Substituting eqn. (A-1.6) the expression for kinetic energy becomes

$$\begin{aligned} Te = \frac{1}{2}\int_o^l \rho A(\dot{U}^2+\dot{V}^2)\, ds + \frac{1}{2}\int_o^l \Big[\rho I(\dot{\theta}_x^2 \cos^2\theta_y + \dot{\theta}_y^2) \\ + I_p\,(\dot{\theta}_x^2 \sin^2\theta_y + \dot{\theta}_z^2 + 2\dot{\theta}_x\dot{\theta}_z \sin\theta_y)\Big]\, ds \end{aligned} \qquad \text{(A-1.8)}$$

Assuming θ_x, θ_y to be small and noting that $\dot{\theta}_z = \Omega_o$(the spin speed of the shaft), the above expression simplifies to

$$Te = \frac{1}{2}\int_o^{\ell} \rho A(\dot{U}^2+\dot{V}^2)\, ds + \frac{1}{2}\int_o^{\ell}\Big[\rho I(\dot{\theta}_x^2 + \dot{\theta}_y^2) + I_p\,(\Omega_o^2 + 2\Omega_o\dot{\theta}_x\,\theta_y)\Big]\, ds \qquad \text{(A-1.9)}$$

REFERENCES

1. Rankine, W.J.M., "Centrifugal Whirling of Shafts", Engineer, Vol. 27, 1869.

2. Loewy, Robert. G. and Piaruli, Vincent. J., "Dynamics of Rotating Shafts", Shock and Vibration Information Centre, United States Debarment of Defence, 1969.

3. Tondl, A., "Some Problems of Rotor Dynamics", Chapman and Hall, London, 1965.

4. Dimentberg, F.M., "Flexural Vibrations of Rotating Shafts", Butterworths, London, 1961.

5. Rao, J.S., "Rotor Dynamics", Wiley Eastern, New Delhi, 1991.

6. Goodwin, W.J., "Dynamics of Rotor-Bearing Systems", Unwin Hyman, London, 1989.

7. Lalane, Michel and Guy, Femaris, "Rotor Dynamics Prediction in Engg.", John Wiley and Sons, New York, 1990.

8. Niordson, F.I., "Dynamics of Rotors", International Symposium, Lingby/Denmark, 1974.

9. e Silva, J.M.M. and da Silva, F.A., "Vibration and Wear in High Speed Rotating Machinery", Proceedings of the NATO advanced study Institution on Vibration and Wear Damage in High Speed Rotating Machinery, Kluwer Academic, London, 1989.

10. Ruhl, R.L. and Booker, J.F., "A Finite Element Model for Distributed Parameter Turbo Systems", J. of Engg. for Industry, Trans. of ASME, Feb. 1972, p. 126.

11. Nelson, H.D. and Mc Vaugh, J.M., "The Dynamics of Rotor-Bearing Systems Using Finite Elements", J. of Engg. for Industry, Trans. of ASME, May 1976, pp. 593-600.

12. Zorzi, E.S. and Nelson, H.D., "Finite Element Simulation of Rotor-Bearing Systems with Internal Damping", J. of Engg. for Power, Trans. of ASME, Jan. 1977, Vol. 71, pp. 71-76.

13. Nelson, H.D., "A Finite Element Rotating Shaft Element Using Timoshenko Beam Theory", J. of Mechanical Design, Trans. of ASME, Oct. 1980, Vol. 102, pp. 793-803.

ME-1992-M-MAT-FLE

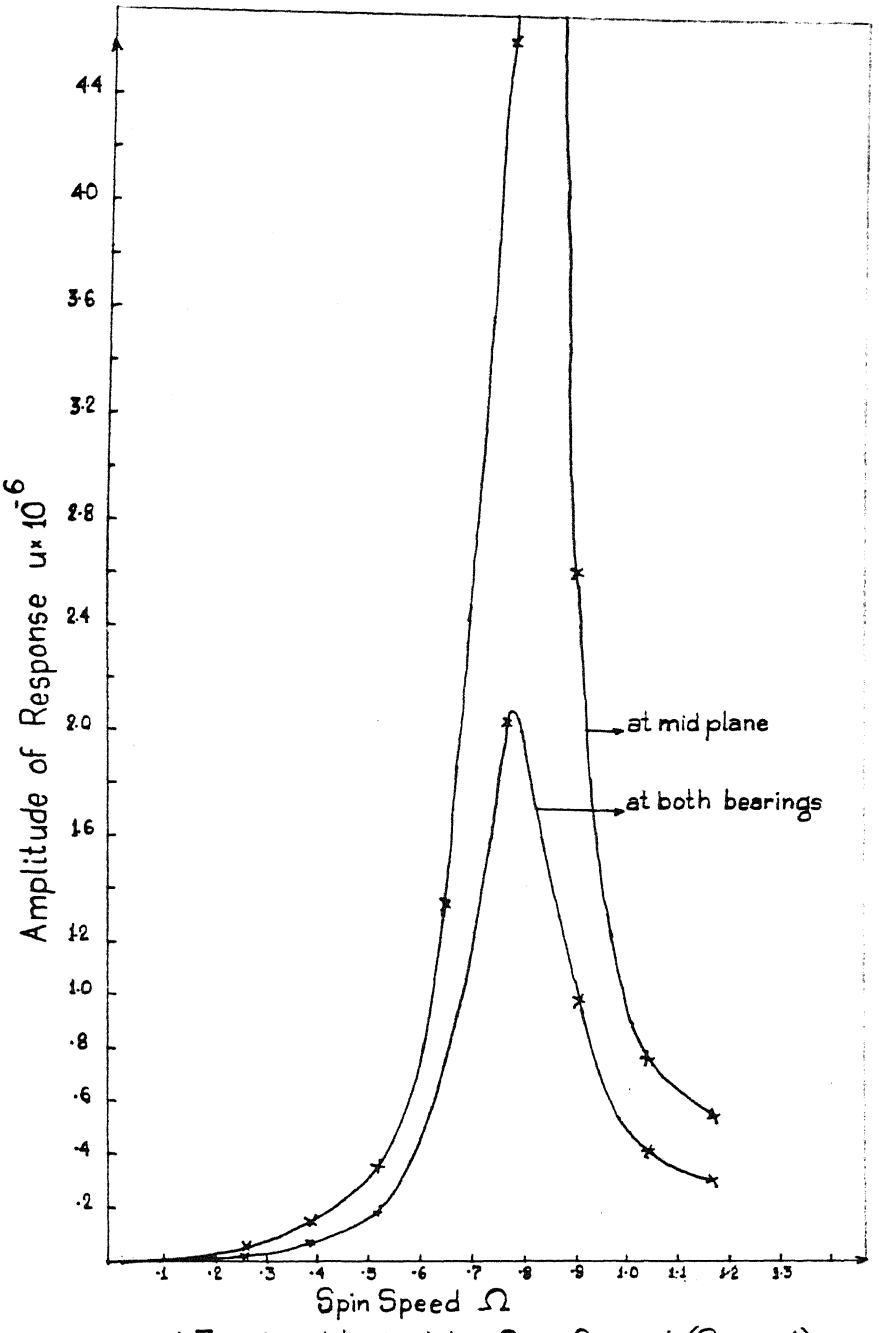

Fig. 4.3 Amplitude Vs Spin Speed (Case 1)

(c) For isotropic bearing properties, the whirl orbit is circular and when bearings are anisotropic the whirl orbit is elliptical as expected.

(d) With damping present, there is a phase shift of response along axial length.

(e) The response is symmetric about mid plane for all cases except Case 5, when the response at a point to the right of mid plane is lower than the corresponding point at left side as expected, as bearing at right hand end is stiffer than the left end one.